Published in final edited form as:
Nat Neurosci. 2016 August ; 19(8): 1050–1059. doi:10.1038/nn.4321.

Zeb2 is essential for Schwann cell differentiation, myelination and nerve repair

Susanne Quintes[#1,2], **Bastian G Brinkmann**[#1], **Madlen Ebert**[1], **Franziska Fröb**[3], **Theresa Kungl**[1], **Friederike A Arlt**[1], **Victor Tarabykin**[4], **Danny Huylebroeck**[5,6], **Dies Meijer**[7], **Ueli Suter**[8], **Michael Wegner**[3], **Michael W Sereda**[1,2,10], and **Klaus-Armin Nave**[1,10]

[1]Max Planck Institute of Experimental Medicine, Department of Neurogenetics, Göttingen, Germany [2]University Medical Center Göttingen (UMG), Department of Clinical Neurophysiology, Göttingen, Germany [3]Institut für Biochemie, Emil-Fischer-Zentrum, Friedrich-Alexander Universität Erlangen-Nürnberg, Erlangen, Germany [4]Institute for Cell and Neurobiology, Center for Anatomy, Charité Universitätsmedizin Berlin, Berlin, Germany [5]Laboratory of Molecular Biology (Celgen), Department of Development and Regeneration, KU Leuven, Leuven, Belgium [6]Department of Cell Biology, Erasmus University Medical Center, Rotterdam, The Netherlands [7]Centre for Neuroregeneration, University of Edinburgh, Edinburgh, United Kingdom [8]Institute of Molecular Health Sciences, Department of Biology, ETH Zürich, Zürich, Switzerland

[#] These authors contributed equally to this work.

Abstract

Schwann cell development and peripheral nerve myelination require the serial expression of transcriptional activators, such as Sox10, Oct6/Scip/Pou3f1 and Egr2/Krox20. Here we show that also transcriptional repression, mediated by the zinc-finger protein *Zeb2*, is essential for differentiation and myelination. Mice lacking *Zeb2* in Schwann cells develop a severe peripheral neuropathy, caused by failure of axonal sorting and virtual absence of myelin membranes. *Zeb2*-deficient Schwann cells continuously express repressors of lineage progression. Moreover, negative regulators of maturation, such as Sox2 and Ednrb, emerge as Zeb2 target genes, supporting its function as an 'inhibitor of inhibitors' in myelination control. When *Zeb2* is deleted in adult mice, Schwann cells readily dedifferentiate following peripheral nerve injury and become

Corresponding Author: Michael W. Sereda, M.D.Department of Neurogenetics Max Planck Institute of Experimental Medicine Hermann-Rein-Straße 3 37075 Göttingen Phone: (0049) (0)551 3899 764 sereda@em.mpg.de.Klaus-Armin Nave, Ph.D. Department of Neurogenetics Max Planck Institute of Experimental Medicine Hermann-Rein-Straße 3 37075 Göttingen Phone: (0049) (0)551 3899 757 nave@em.mpg.de.
[10]These two authors jointly directed the study

Accession codes

Microarray data have been deposited in NCBI Gene Expression Omnibus under accession code GSE76027.

Author contributions

S.Q. and B.G.B. designed the study, performed experiments and wrote the manuscript. M.E., T.K., and F.A.A. contributed to experiments. F.F. performed luciferase assays. V.T., D.H., D.M., and U.S. provided transgenic mice. M.W. supervised F.F. and contributed to discussions. M.W.S. and K.A.N. contributed to the manuscript and supervised the study.

Competing financial interests

The authors declare no competing financial interests.

Europe PMC Funders Author Manuscripts

'repair cells'. However, nerve regeneration and remyelination are both perturbed, demonstrating that Zeb2, although undetectable in adult Schwann cells, has a latent function throughout life.

Introduction

The successive developmental stages of Schwann cell proliferation, axon sorting and myelination are regulated by a feed-forward cascade of transcriptional activators that ultimately up-regulate a large number of genes encoding myelination-associated enzymes and myelin structural proteins1–3. Well studied examples include the transcription factor Krox20 (Egr2), as illustrated by Krox20 mutant Schwann cells, which successfully sort axons but fail to generate or maintain myelin membranes4,5. Also the transcription factors Oct6 and Sox10, developmentally upstream and directly interacting with Krox20 promote Schwann cell differentiation and myelination6,7. Studies on constitutive and conditional Sox10 mutant mice revealed an essential role of this transcription factor in Schwann cell specification, lineage progression, differentiation, myelin formation and maintenance8,9,10,11.

Most research on the genetic control of Schwann cell differentiation has concentrated on transcriptional activators that would generate positive feed-forward loops when uncontrolled. This raises the question how Schwann cell differentiation is properly balanced. Transcriptional repressors are plausible candidates. For example, the co-repressor Nab (NGFI-A/Egr-binding) is essential for PNS myelination12. However, when associated with Krox20 this protein is a co-activator of myelin protein genes, and the significance of gene repression by Nab/Krox20 complexes in Schwann cells is unclear13,14. Also the zinc-finger protein Yin-Yang 1 (*Yy1*), an essential transcriptional inhibitor in myelinating oligodendrocytes15, has so far only been characterized as a transcriptional activator in the peripheral nervous system (PNS), immediately upstream of Krox20 (Ref.16). Other transcription factors have been functionally identified as "negative regulators" of myelination, but these include both transcriptional activators (e.g. Sox2, c-Jun, Pax3, Notch-ICD) and inhibitors (Id2). While the most likely function of these factors is driving Schwann cell "de-differentiation" after injury and in preparation for nerve repair1, their presence interferes with myelination and myelin maintenance.

Zinc Finger E-Box Binding Homeobox 2 (*Zeb2*, also known as *Sip1* or *Zfhx1b*) is a widely expressed zinc-finger homeobox protein, originally identified by its binding to Smad1 (Ref. 17,18). During epithelial to mesenchymal transition, Zeb2 represses the transcription of several genes for cell adhesion molecules, such as E-cadherin19–21. In the central nervous system, newly born neurons express Zeb2 to down-regulate signalling proteins that drive neurogenesis of adjacent precursors22. Zeb2 also regulates oligodendrocyte differentiation, because mutant cells fail to fully mature and make myelin23.

Similar to Sox10, Zeb2 is also detectable early in the neural crest lineage24 and therefore a plausible candidate for transcriptional regulation in the Schwann cell lineage. In humans, mutations of Sox10 and Zeb2 have been associated with the clinically related Waardenburg syndrome type 4 and Mowat-Wilson syndrome, respectively25. For neural crest cells, even direct interactions of Sox10 and Zeb2 proteins have been proposed, but this is again difficult

Europe PMC Funders Author Manuscripts

to reconcile with their respective roles as transcriptional activators and repressors26. Zeb2 is a canonical transcriptional repressor and in neural crest-derived immature Schwann cells a candidate to 'release the brake' on differentiation that might be imposed by negative regulators, such as Sox2.

Here, we show that *Zeb2* targets are indeed inhibitors of Schwann cell differentiation. Mice lacking *Zeb2* specifically in this lineage show a complete arrest of Schwann cell maturation and exhibit a virtually myelin-deficient phenotype. However, *Zeb2*-deficient Schwann cells survive *in vivo* and maintain axonal integrity. While Zeb2 is not required for adult myelin maintenance and axonal integrity, after injury *Zeb2*-deficient Schwann cells fail to efficiently support nerve regeneration.

Results

Zeb2 is expressed in Schwann cell development and after injury

To explore Zeb2 expression by Schwann cells, we immunostained paraffin sections of mouse sciatic nerves at different developmental stages. Zeb2 was exclusively localized to cell nuclei. At E18.5, about 90% of Schwann cells were Zeb2-positive. At age P10, roughly 70% of cells could be immunostained, and in adult mice virtually all Schwann cells were Zeb2-negative (Fig. 1a).

To study the Schwann cell-specific function of Zeb2, we bred *Zeb2* floxed mice27 to mice expressing Cre under control of the *desert hedgehog* promoter, leading to recombination in the Schwann cell lineage between embryonic days (E) 11 and 13.5 (Ref. 9,28), when most cells are at the precursor stage29. Loss of Zeb2 protein was confirmed by the absence of immunostaining (Fig. 1a) and by analysis of steady-state mRNA levels in sciatic nerve at age P1 (reduction to 14.1% of control, data not shown).

To determine possible Zeb2 re-expression in Schwann cells after acute sciatic nerve injury, we stained paraffin sections of the distal segment at different time points after a nerve crush (Fig. 1b). Zeb2 was detected as early as six hours after injury (data not shown) and 7 days after injury 80% of all cells could be stained (Fig. 1b). On day 14 after crush, a time point when remyelination is at its peak, about 50% percent of all Schwann cells still expressed Zeb2 (Fig. 1b). Zeb2 was absent from distal stumps 28 days after crush (Fig. 1b) and we could not detect Zeb2-positive cells in the contralateral uninjured nerve (Fig. 1b). We conclude that Zeb2 expression is transient in peripheral nerves, preceding myelination in development and remyelination after acute nerve injury.

Zeb2 in Schwann cells is essential for axon sorting and myelination

Conditional mutants (*Dhh-cre::Zeb2*$^{flox/flox}$) were born at the expected Mendelian ratio and phenotypically distinguishable from littermate controls in the second postnatal week, when they had reduced body size and developed ataxia and hind limb weakness (Supplementary Video 1). The latter progressed with age but never led to complete hind limb paralysis. Surprisingly, when electrically stimulating the sciatic nerve of conditional mutants it was difficult to record compound muscle action potentials (CMAP) as in heterozygous controls

(Fig. 1f), which suggests major conduction blocks. However, *Zeb2* conditional mutants had a normal life span, and we only occasionally observed unexplained premature deaths.

To assess the developmental stage of *Zeb2*-deficient Schwann cells, we immunostained cross-sections from mutants and controls for Krox20 (also known as *Egr2*) and Sox2, as prototype positive and negative regulators, respectively. S100β was taken as a marker for both, immature and mature Schwann cells. While Schwann cells in control mice robustly expressed Krox20 and S100β and were negative for Sox2, only a few *Zeb2*-deficient Schwann cells expressed Krox20 and S100β but about 30 percent were positive for Sox2 (Fig. 1c-e).

At P25, the sciatic nerves of mutant mice were thinner and more translucent than those of controls (Fig. 2a,b). Immunostaining of cross-sections for axonal β–Tubulin (TuJ1) and myelin basic protein (Mbp) revealed closely packed, amyelinated axons in mutants but not in controls (Fig. 2c,d). Also by electron microscopy, *Zeb2*-deficient mice lacked peripheral myelination and revealed abnormal axon bundles, with Schwann cells engulfing larger groups of axons that also greatly varied in diameter (Fig. 2e-i). Within these bundles, interdigitating Schwann cell processes could be observed, but the majority of axons remained closely packed, resembling axons associated with immature Schwann cells in embryonic nerves (Fig. 2i). Most Schwann cells failed to establish the one-to-one relationship with axons. We noticed that the basal lamina of *Zeb2*-deficient Schwann cells was often thin, discontinuous, and not attached to the glial cell membrane, providing a plausible cause of failed axonal sorting30. Many Schwann cells displayed also 'redundant basal lamina loops' (Fig. 2g, red arrow heads).

At one year of age, peripheral axons had grown in diameter, but the overall pathology appeared unchanged (Fig. 2j-m). Compared to P25, the total Schwann cell number was unaltered in mutants (Supplementary Fig. 1a). In agreement, the percentage of BrdU-positive (proliferating) cells did not differ between mutants and controls at E18.5, P10 and P25 (Supplementary Fig. 1b). This suggests, that *Zeb2*-deficient Schwann cells exit the cell cycle normally and survive in the absence of myelination.

At all time points studied (including 1 year of age) we found no evidence for axonal degeneration, except for rare axonal swellings (not shown). At one year, the total number of axons was unaltered in mutants compared to controls (Supplementary Fig. 1c,d). This suggests that *Zeb2*-deficient Schwann cells can support axon survival despite a dysmyelination that causes conduction blocks.

Mutant SC express negative regulators of differentiation

To further define the stage at which *Zeb2*-deficient Schwann cells arrest in development, we performed a transcriptome analysis of sciatic nerves at age P25. Steady-state levels of more than 700 mRNAs differed (at least 2-fold) in abundance between the two genotypes. The 20 top up- and down-regulated genes are shown in Fig. 3a. We confirmed a subset of differentially regulated genes by quantitative real-time PCR, selecting promyelinating factors as well as negative regulators of myelination (note the logarithmic scale in Fig. 3b,c). As predicted from the phenotype of *Zeb2*-conditional mutants and the histological analysis,

genes encoding myelin proteins were down-regulated in mutants compared to controls (Fig. 3c). This was also the case for promyelinating factors of PNS myelination, such as Oct6/SCIP and Krox20/Egr2 (Fig. 3c). Importantly, *Zeb2*-deficient Schwann cells revealed the persistent expression of transcripts that are normally down-regulated at this age, (Fig. 3b). This includes transcripts for negative regulators of Schwann cell differentiation (e.g. Sox2, c-Jun, Id2) and markers defining immature Schwann cells (e.g. Gfap). Zeb2-deficient Schwann cells also expressed very low amounts of S100β, a well-known marker of both immature and mature Schwann cells (Fig. 3c). In addition, we identified the Notch effector Hey2 as one of the most strongly (16.7±1.4-fold) upregulated genes in our data set (Fig. 3a,b), as confirmed by quantitative PCR. Also other components of the Notch signaling cascade were upregulated in our microarray analysis in mutants compared to controls, such as Notch1 (1.3-fold), Hes1 (1.6-fold) and Jagged1 (1.9-fold), arguing for persistently activated, inhibitory Notch signaling in *Zeb2*-deficient Schwann cells. We also found and confirmed by RT-PCR highly elevated (13.4±3.1-fold) expression of the endothelin receptor B (Ednrb) gene (Fig. 3b), encoding an efficient repressor of Schwann cell differentiation upon ligand binding31. Taken together, *Zeb2*-deficient Schwann cells are arrested at an early developmental stage, with a very low expression of maturation factors and persistent (abnormal) expression of several negative regulators.

SC Zeb2 represses negative regulators of differentiation

To test whether Zeb2 acts as a repressor of relevant target genes, we performed luciferase gene reporter assays using the S16 Schwann cell line (Fig 3d). Promoter regions of murine *Sox2*, *Hey2* and *Ednrb,* each containing putative Zeb2 binding sites [CACCT(G)], schematically depicted in Fig. 3e, were cloned into the pGL2-luciferase plasmid and co-transfected with increasing amounts of a Zeb2 expression plasmid into S16 cells. This led to a significant dose-dependent downregulation of luciferase activity when compared to co-transfection with empty pCMV5 plasmid set to 100% (Fig. 3d). To confirm the interaction of Zeb2 and its target genes at the DNA level, we performed chromatin immunoprecipitation (ChIP) experiments using pooled sciatic nerves from 1 day old wildtype mice. By qPCR we detected an enrichment of amplified fragments from the promoters of all three target genes (Sox2, Hey2, and Ednrb) that contained the canonical Zeb2 binding site, compared to control ChIP experiments without Zeb2 antibody (Supplementary Fig. 2). A DNA fragment of a *bona fide* target gene (*Cdh1*) lacking a Zeb2 recognition site was used as a negative control.

Zeb2-mediated repression of Ednrb and Hey2 in SC *in vivo*

To determine whether Zeb2-mediated 'inhibition of inhibitors' is also functionally relevant *in vivo,* we generated double mutant mice, i.e. mice that combine *Zeb2* deletion with the loss of either *Ednrb* or *Hey2*, for which floxed mutants were available32,33. By crossbreeding, we obtained two genotypes (*Dhh-cre::Zeb2*$^{flox/flox}$*::Ednrb*$^{flox/flox}$ and *Dhh-cre::Zeb2*$^{flox/flox}$*::Hey2*$^{flox/flox}$), termed Zeb2/Ednrb-dcKO and Zeb2/Hey2-dcKO in the following. As a phenotypical "rescue" was not expected with the loss of only one inhibitor, we searched for histological signs of improvement in these double-mutants. We immunostained cross sections of sciatic nerves for Krox20. As shown above (Fig. 1c), the number of labelled Schwann cell nuclei (in *Zeb2*$^{fl/fl}$ controls 36.7±2.9 per section) was

strongly reduced in *Zeb2* single mutants (to 6.0±0.4), but increased significantly both in Zeb2/Ednrb-dcKO (to 19.9±4.3) and in Zeb2/Hey2-dcKO (to 16.8±2.9) sciatic nerves (Fig. 4a,b).

Also at the morphological level, axon-Schwann cell units appeared more mature in Zeb2/Ednrb and in Zeb2/Hey2 conditional double-mutants, at least when compared to the large and unsorted fiber bundles of Zeb2 single mutants (Fig. 4c). The number of Remak-like (partially sorted) bundles with only 1-5 axons at age P25 (Fig. 4d) was higher in sciatic nerve cross sections of double mutants (Zeb2/Ednrb*:* 51.1±18.85 %; Zeb2/Hey2: 55.2±13.49 %) than Zeb2 single mutants (*Dhh-cre::Zeb2*$^{fl/fl}$: 27.5±6.1 %). Thus, already the lack of one negative regulator (downstream of Zeb2) improves the ability of *Zeb2* mutant Schwann cells to initiate axon sorting. To further characterize Zeb2/Ednrb and Zeb2/Hey2 mutants, we analyzed target gene expression in sciatic nerves at age P25 (Fig. 4e-g). We could not detect a change of Sox2 or Hey2 mRNA in Zeb2/Ednrb-dcKO mice in comparison to respective controls (Fig. 4e and g). However, Sox2 levels were significantly lower in Zeb2/Hey2-dcKO mice than in *Dhh-cre::Zeb2*$^{fl/fl}$ mice and were comparable to *Zeb2*$^{fl/fl}$ mice (Fig. 4e). Also Ednrb was significantly downregulated in comparison to *Zeb2*$^{fl/fl}$ single mutants (Fig. 4f).

Zeb2-deficient SC fail to efficiently support regeneration

Since Schwann cells reexpressed Zeb2 after an acute nerve injury (Fig.1b), we asked whether the induction of Schwann cell de-differentiation and peripheral nerve regeneration would be affected by the absence of Zeb2. To this end we inactivated *Zeb2* in Schwann cells of adult mice, using a tamoxifen-inducible *Plp-creERT2* driver line34. Recombination was induced at 6-8 weeks of age and efficient CreERT2 expression was confirmed, using a Cre-sensitive tdTomato reporter allele35, on sciatic nerve cryostat sections (Suppl. Fig. 3).

When *Plp-creERT2::Zeb2*$^{fl/fl}$ mice were analysed 12 weeks after the last tamoxifen injection, sciatic nerve morphology and myelin sheath thickness appeared unaltered (Supplementary Fig. 4a, b). We then performed sciatic nerve crushes in mice 4 weeks after the last tamoxifen (or vehicle) injection. Footprint sequences of walking mice were used to monitor functional recovery. For histological analyses, animals were sacrificed 11, 28 and 56 days after sciatic nerve crush. In these experiments, mice from the three control groups functionally recovered as expected and as measured by the sciatic functional index. However, *Plp-creERT2::Zeb2*$^{fl/fl}$ mice remained severely impaired until the end of this study (56 days after crush, Fig. 5a).

In physiological tests, carried out 52 days after sciatic nerve crush, *Zeb2*-floxed control mice regained significant motor nerve conduction. We recorded a velocity (NCV) of about 18±2.9 m/s, which is about 54% of the NCV of an unharmed contralateral nerve (33±5.2 m/s), as determined in mice of either genotype.

In contrast, *Zeb2* conditional mutants maintained severe axonal conduction problems that did not allow us to measure a NCV (Fig. 5b,c). Distal amplitudes (normal contralateral nerve: 29.8±10.1 mV) were still reduced 52 days after crush injury in control mice (10.9±4.4

mV) and undetectable in *Plp-creERT2::Zeb2*$^{fl/fl}$ mutants, indicating a regeneration failure with irreversible conduction blocks (Fig. 5d).

Indeed, when we immunostained sciatic nerve cross sections for myelin (Mbp) and axons (TuJ1), virtually all fibers showed remyelination in control mice (Fig. 6a, top panel), whereas in nerves of tamoxifen-induced *Plp-creERT2::Zeb2*$^{fl/fl}$ mutants we observed large amyelinated fibers 8 weeks after injury (Fig. 6a, bottom panel, white arrow heads). We also analysed remyelination by electron microscopy (Fig. 6b, c, e). At 28 days and 56 days after crush injury mutants exhibited significantly fewer remyelinated axons (Fig. 6d, e and Supplementary Fig. 5a).

Interestingly, by G-ratio analysis remyelinated axons in mutant (*Plp-creERT2::Zeb2*$^{fl/fl}$) mice had the same myelin sheath thickness that we determined in controls (Supplementary Fig. 5b). Also 56 days after crush, we still observed remyelinating Schwann cells with fewer, non-compacted myelin loops (Fig. 6b). Thus, the timing of Zeb2 re-expression after acute nerve trauma (Fig. 1b) and the defect of remyelination in mutant mice strongly suggest Zeb2 is key to the efficient Schwann cell response upon nerve injury.

Zeb2-deficient SC do not fully redifferentiate after injury

To distinguish between alternative Zeb2 functions after nerve injury, we first studied sciatic nerves in tamoxifen-treated *Plp-creERT2::Zeb2*$^{fl/fl}$ mice 3 days after transection, a time point at which Schwann cell de-differentiation is at its peak. At this time, there was no significant difference in the number of residual myelin sheaths (1650±89 per section), when compared with vehicle-treated controls (1785±287) 3.0 mm distal to the transection site (Fig. 7a,b). We also detected no significant difference in the number of c-Jun-positive nuclei between two control groups and tamoxifen-treated mutants in distal segments of sciatic nerves 3 days after crush injury (Fig. 7 c,d).

Moreover, steady-state mRNA levels of Schwann cell dedifferentiation markers1, such as c-Jun, Sox2 and Ngfr were comparable in the distal stump (Fig. 7e and data not shown), whereas myelination markers, such as Krox20 and Mpz, were downregulated in both, mutants and controls, when compared to the contralateral nerve (Fig. 7e). Taken together, the early steps of Schwann cell dedifferentiation are not perturbed by the lack of Zeb2.

We next analysed at a functional level the regenerative axon outgrowth of crushed sciatic nerves in conditional *Zeb2* mutants and controls, using the "pinch test". When tested 4 days after injury, deeply anaesthetized mice of all three control groups showed a clear muscle reaction to a pinch of the sciatic nerve applied with a pair of forceps distal to the original crush site (Fig. 7f). However, the distance at which a response could be elicited differed between genotypes, indicating more efficient axon outgrowth in all control groups (e.g. 6.6±0.8 mm in mice lacking Cre) compared to tamoxifen-treated *Zeb2* mutants (5.4±1.3 mm).

We hypothesized, that reduced regenerative capacity is caused by poor Schwann cell differentiation. We therefore analysed the distal stump of sciatic nerves at a late time point (56 days after crush), when control mice had fully recovered. Indeed, in *Zeb2* mutants we

could still detect a significant expression of dedifferentiation markers, such as Sox2 and Id2 (Fig. 7g). Interestingly, Hey2 mRNA was only upregulated in mutant nerves (Fig. 7g) (i.e. "ectopic" expression similar to that found in *Zeb2*-deficient Schwann cells at age P25). In contrast, Krox20 was downregulated only in mutant nerves (in comparison to the sustained expression in uninjured nerves), whereas Oct6 expression levels were similar in mutants and controls (Fig. 7g). Taken together, *Zeb2*-deficient Schwann cells can dedifferentiate after injury, but fail to redifferentiate and provide efficient myelin repair.

Discussion

We have identified an essential regulator of Schwann cell differentiation and peripheral myelination, the two-handed zinc finger/homeodomain protein Zeb2. In contrast to previously described promyelinating transcription factors in the Schwann cell lineage, such as Oct6, Krox20 and Sox10, which activate the transcription of down-stream factors and ultimately myelin-associated genes, Zeb2 is widely expressed17 and a transcriptional repressor in Schwann cells. These findings are in agreement with the work of Wu et al. (36, this issue).

Null mutant mice of *Sox10*, a gene which is like *Zeb2* already expressed in the emerging neural crest, die embryonically with a lack of peripheral glia8. Only later cell-specific deletion of *Sox10* after Schwann cell specification (induced by *Dhh-cre* as in *Zeb2* cKO) leads to a similar developmental arrest in peripheral nerves with a lack of radial axonal sorting and virtual absence of myelin9.

Early arrest of Schwann cell maturation has been observed before in the context of chromatin remodelling. Mice in which Schwann cells lack *Brg1*, a subunit of the BAF chromatin-remodelling complex that is recruited by Sox10, develop a severe peripheral neuropathy and die prematurely37. Whereas the morphological defects of dysmyelination are strikingly similar in conditional *Dhh-cre*::*Sox10*, *Dhh-cre*::*Brg1* and *Dhh-cre*::*Zeb2* mutant mice, it is surprising that in *Zeb2*-deficient mice all Schwann cells survive. Despite the virtual absence of myelin and similarly severe neuropathy, conditional *Zeb2* mutant mice have a normal life span, and *Zeb2*-deficient Schwann cells support axon survival. Apparently the (ancestral) function of axon ensheathing glial cells in providing metabolic support is maintained.

We also note that in *Zeb2*-deficient Schwann cells Sox10 mRNA itself is unaltered in abundance (data not shown). The transcriptional (co-) activator Sox10 is expressed throughout the Schwann cell lineage and directly binds to Oct6 and Krox20, potentially affecting a broader set of myelin-associated genes6, including most likely those that are required for survival and axonal metabolic support. We speculate that Schwann cell-mediated axonal support, which protects from complete paralysis and lethal breathing defects is largely independent of Zeb2.

The developmental defect of conditional *Zeb2* mutant mice is more severe than that of *Oct6* or *Krox20* mutants. Deletion of *Oct6* causes only a transient arrest of Schwann cell

differentiation after radial sorting, i.e. at the pro-myelin stage38,39. Likewise, Schwann cells lacking *Krox20* are able to sort axons but then completely fail to myelinate4.

Considering the unaltered levels of Sox10 mRNA in *Zeb2*-deficient Schwann cells and the more severe phenotype than that observed in *Krox20* null mice, the most likely explanation why conditional *Zeb2* mutants display very low expression of Krox20 and myelin protein genes is not the absence of pro-myelin factors, but the persistent presence of maturation inhibitors (e.g. Sox2, c-Jun, Ednrb) and the resulting developmental arrest. However, we cannot formally exclude that also transcriptional activation of unknown target genes by Zeb2 (e.g. in combination with unknown coactivators) promotes Schwann cell differentiation in wild-type mice. Details of the transcriptional repression mechanisms by Zeb2 remain to be determined. One possibility is an interaction of Zeb2 with the HDAC1/2-NuRD corepressor complex40 in Schwann cells36.

With their radial sorting defect conditional *Zeb2* mutants resemble mutants of basal lamina signaling, such as beta-1 integrin/dystroglycan conditional mutants 41 or laminin 2/8 double knockout mice 42. In conditional *Zeb2* mutants, the basal lamina is thin, disorganized and often discontinuous. In DRG cocultures *Zeb2*-deficient Schwann cells failed to myelinate also when provided with an artificial basal lamina (data not shown). Thus, basal lamina abnormalities are likely a secondary defect of *Zeb2*-deficient Schwann cells rather than the cause of dysmyelination.

We observed very low levels of S100β mRNA and protein in *Zeb2*-deficient Schwann cells. This could mean, that they are arrested even before reaching the immature developmental stage. However, this is unlikely, as we did not observe significantly increased Schwann cell proliferation or apoptosis.

The hierarchical relationship of the known transcription factors in the Schwann cell lineage is complex, owing in part to their broad temporal expression domains and changing molecular interactions, including positive feedback loops3. For example, Krox20 is activated in pro-myelinating Schwann cells by the positive regulators Oct6 and Sox10, which then collectively upregulate genes for myelin proteins and enzymes of the lipid biosynthesis pathway. How are these feed-forward loops developmentally controlled? Our data on Zeb2 suggest the existence of several brakes in the system, with the loss of Zeb2 leading to continous expression of developmental inhibitors that block axonal sorting and myelination. This group of negative regulators is overlapping but not identical to other factors known to drive programmed de-differentiation of mature Schwann cells, such as c-Jun, after nerve injury (see below).

By expression profiling of peripheral nerves from *Zeb2* mutant mice and by functional analysis of different promoter-reporter constructs we have identified Ednrb, Sox2 and Hey2 *as* target genes of Zeb2. We have selected these genes from a much larger group of abnormally up-regulated genes in order to show proof-of-principle for transcriptional repression by Zeb2, as well as for their putative inhibitory function in Schwann cell differentiation. Two of these genes had been previously associated with the Schwann cell lineage. The endothelin B receptor (Ednrb) localizes to the plasma membrane of Schwann

cell precursors and, upon binding of endothelin, delays the generation of immature Schwann cells, both *in vitro* and *in vivo.* Indeed, *Ednrb* null mutant Schwann cells differentiate earlier than normal as shown by premature S100β expression 31.

Sox2 is also a member of the Sry-related HMG box familiy of transcription factors, but (unlike Sox10) widely expressed. Sox2 is down-regulated early in Schwann cell development, coinciding with Krox20 expression 43. Recently, it has been shown that overexpression of Sox2 (a transcriptional activator) leads to persistent proliferation of Schwann cells and inhibits myelination, implicating Sox2 as a negative regulator of Schwann cell maturation *in vivo* (D.B. Parkinson, personal communication).

Hey2, a member of the hairy and enhancer-of-split related bHLH transcription factor family, recruits histone deacetylases to repress transcription and acts as a downstream effector of Notch signalling44. Notch signaling serves as a timer in the generation of immature Schwann cells from precursors and is down-regulated in cells that express Krox20. Additionally, Notch acts as an inhibitor of myelination *in vitro* and *in vivo* and is reexpressed in the distal stump of cut nerves 45.

In our analysis, Hey2 is expressed at low levels in adult nerves, and not activated during injury-induced Schwann cell de-differentiation (Fig. 7d and data not shown). We therefore found Hey2 amongst the most highly up-regulated mRNAs in sciatic nerves of *Dhh-cre::Zeb2*$^{fl/fl}$ mice at age P25. Moreover, Hey2 was strongly expressed in adult mutants 8 weeks after nerve injury. In both cases, "ectopic induction" of Hey2 was a special feature of *Zeb2*-deficient Schwann cells. The physiological function of Hey2 in the Schwann cell lineage remains unknown. Conditional *Dhh-cre::Hey2*$^{flox/flox}$ single mutants that we created in the course of our "rescue" experiments were normally developed and myelinated (data not shown).

Thus, our findings suggest that negative regulatory proteins such as Sox2, Hey2, or Ednrb need to be down-regulated early in development in order for Schwann cell differentiation, axonal sorting and myelination to proceed (schematically depicted as a model in Supplementary Fig. 6). Since Zeb2 itself is only transiently expressed, the down-regulation of its target genes ("inhibiting the inhibitors") most likely allows immature Schwann cells to overcome a developmental block, after which their further differentiation becomes Zeb2-independent. At least two of the identified Zeb2 target genes appear to contribute to this block (*Hey2* and *Ednrb*) as evident from the partial rescue in corresponding double-mutant mice. One cannot assume that the phenotype of *Zeb2* mutant mice can be "rescued" by introducing a second mutation into one gene for a (de-repressed) inhibitor. It is thus surprising that the additional deletion of either *Ednrb* or *Hey2* was sufficient to markedly increase the number of Krox20-positive Schwann cells and morphological signs of sorting (more bundles with only 1-5 axons) in corresponding double-mutant mice. Experiments to find out whether these effects can be strengthened by targeting yet other genes and combining them in triple and quadruple mutants are important but beyond the scope of this first report.

Normally myelinated (adult wild-type) nerves, exhibit the absence of both Zeb2 and its repressed target gene product(s), strongly suggesting that other factors are responsible to maintain the brake on the expression of inhibitors, which would otherwise trigger de-differentiation. The identity of these repressors is not known. At the same time, myelin maintenance has been shown to depend on continuous expression of the pro-myelinating factors Sox10 and Krox20 (Ref.5,11).

Mutations of the human *Zeb2* gene cause the rare Mowat-Wilson syndrome, characterized by moderate to severe mental retardation, brain abnormalities and variable features including Hirschsprung disease25. A reduced response to nociceptive stimuli has been found in patients affected by Mowat-Wilson syndrome46 and lowered pain sensitivity and reduced number of nociceptive C-fibers has been demonstrated in *Zeb2* heterozygous null mice47. However, it is unclear whether the reduced pain response seen in some Mowat-Wilson patients is a peripheral neuropathy or CNS phenotype46.

In the CNS, myelination by oligodendrocytes is controlled in many ways by negative regulators. Direct interactions with signaling molecules, such as bone morphogenetic protein (BMP), Notch ligand, or Wnt proteins, can inhibit gene expression48. At the molecular level, chromatin remodelling and epigenetic silencing of transcriptional repressors also follows the principle "inhibiting the inhibitors" 49. In oligodendrocyte development, Zeb2 is also expressed, activated by Olig1 and Olig2, and essential for CNS myelination, as illustrated in *Olig-cre::Zeb2*$^{flox/flox}$ mice23. Zeb2 levels are low in oligodendrocyte precursors (OPC) and high in mature oligodendrocytes, where Zeb2 serves a dual role not only as a repressor, but also as a transcriptional activator of the *Smad7* gene. It is the lack of Smad7, which contributes to failed OPC differentiation and CNS dysmyelination in conditional mutant mice23. Thus, despite some phenotypical resemblence, Zeb2 serves different functions in PNS and CNS glial development.

When we deleted *Zeb2* in Schwann cells of adult mice we found a severe delay in regeneration and functional recovery after sciatic nerve crush injury. Even after eight weeks remyelination was not complete. Such a dramatic failure of myelin repair has been described in mice lacking the AP1 transcription factor c-Jun in Schwann cells50. However, in *c-Jun* mutant mice, already the formation of a functional 'repair cell' is impaired, while in *Zeb2* conditional mutants, repair cells are generated but redifferentiation is inefficient. After sciatic nerve crush, Schwann cells lacking *c-Jun* fail to form regenerative tracts (Bands of Bungner), which leads to a dramatic reduction of axon outgrowth50. Here, we only detected a minor reduction in axon outgrowth when tested 4 days after crush (Fig. 7e). Interestingly, in *Zeb2* conditional mutants (and similar to *c-Jun* conditional mutants), if remyelination does initiate myelin repair proceeds normally, as determined by G-ratio analysis. It has been hypothesized that the 'repair cell' marks dedifferentiation beyond the immature Schwann cell stage50. One analysis of injured nerves even revealed Schwann cell-derived melanocytes, normally a distinct sublineage of precursor cells51.

Repair cells that form after nerve injury, and which are dependent on factors such as Zeb2 to fully activate the Schwann cell redifferentiation program, are an important feature of nervous system function. Further characterization of genes involved in the plasticity of Schwann

cells during development and in injury-related redifferentiation at adult stages will help to better understand the outcome of human demyelinating neuropathies and other diseases of the peripheral nervous system.

Online Methods

Animals

All experiments involving mice were conducted according to the Lower Saxony State regulations for the use of experimental animals in Germany as approved by the Niedersächsisches Landesamt für Verbraucherschutz und Lebensmittelsicherheit (LAVES) and performed in compliance with the animal policies of the Max Planck Institute of Experimental Medicine. Mice were group-housed in individually vented cages with a 12 hour light/dark cycle. Male and female mice were included in all experiments and randomly assigned to experimental groups according to age and genotype. *Zeb2*$^{fl/fl}$ mice27 were bred to *Dhh-cre* transgenic mice28. *Dhh-cre::Zeb2*$^{fl/fl}$*::Ednrb*$^{fl/fl}$ mice were generated by breeding *Dhh-cre::Zeb2*$^{fl/+}$*::Ednrb*$^{fl/fl}$ mice to *Zeb2*$^{fl/fl}$*::Ednrb*$^{fl/fl}$ mice32. Floxed Hey2 mice33 were acquired from Jackson laboratories. *Dhh-cre::Zeb2*$^{fl/fl}$*::Hey2*$^{fl/fl}$ mice were generated by breeding *Dhh-cre::Zeb2*$^{fl/+}$*::Hey2*$^{fl/fl}$ mice to *Zeb2*$^{fl/fl}$*::Hey2*$^{fl/fl}$ mice. Floxed (double floxed) littermates were used as experimental controls in all experiments unless indicated otherwise. *PLP-creERT2::Zeb2*$^{fl/fl}$ mice were generated by breeding Zeb2$^{fl/fl}$ mice to *PLP-creERT2* mice34. *Zeb2* floxed mice, *Hey2* floxed mice, *PLP-creERT2* mice, and *Dhh-cre* mice were on C57/Black6N background, *Ednrb* floxed mice were on mixed C57Bl/6-SV129 background. Genotyping was performed on DNA isolated from tail or ear biopsies according to routine PCR methods using the following primers: Dhh-cre sense 5'-CCTGCGGAGATGCCCAATTG-3' antisense 5'-CAGCCCGGACCGACGATGAA-3' Zeb2 floxed sense 5'-TGGACAGGAACTTGCATATGCT-3' anti-sense 5'-GTGGACTCTACATTCTAGATGC-3' Hey2 floxed sense 5'-CTAGAGAGG ACCTGGAGAGTTTAAG-3' antisense 5'-CTGTGCCACCAGCCTTAAAACC-3' Ednrb wild type allele sense 5'-CTGAGGAGAGCCTGATTGTGCCAC-3' antisense 5'-CGACTCCAAGAAGCAACAGCTCG -3' Ednrb floxed allele sense 5'-TGGAATGTGTGCGAGGCC -3' Ednrb floxed allele antisense 5'-CAGCCAGAACCACAGAGACCACCC -3' PLPCreERT2 transgene sense 5'-TGGACAGCTGGGACAAAGTAAGC -3' antisense 5'-CGTTGCATCGACCGGTAATGCAGGC -3'.

Cell lines

The S16 cell line was directly obtained from the producer Richard H. Quarles 52 at early passages. Identity of the cells was confirmed by PCR. The cell line was not tested for mycoplasma contamination.

Statistics

In box-whisker-blots whiskers show the minimum and maximum, boxes extend from the first to the third quartiles with cross lines at the median. In dot blots, dots represent individual experiments or animals with cross lines at the mean +/- SD or SEM as indicated in the respective figure legends. When comparing two groups, statistics were performed

using the two-tailed Student's t-test for unpaired samples assuming unequal variance. When comparing multiple groups, one-way ANOVA was performed except for experiments where n=3, where Kruskall-Wallis one-way ANOVA was chosen. P values below 0,05 were considered significant (* <0.05; ** <0.01; *** <0.001). No statistical tests were used to pre-determine sample sizes, but our sample sizes are similar to those generally employed in the field. Normal distribution of data was assumed, but not formally tested. All statistical analyses were performed using GraphPad Prism 6.00 or Microsoft Excel. A supplementary methods checklist is available.

Induction of recombination, surgical procedures and foot print analysis

PLP-creERT2::Zeb2$^{fl/fl}$ mice and Zeb2$^{fl/fl}$mice were treated at the age of 6-8 weeks twice for 5 consecutive days with one daily intraperitoneal injection of 1 mg tamoxifen in corn oil with 10% analytical ethanol (all from Sigma) or the corn oil/ethanol mixture only (vehicle). Sciatic nerve crush or transection was performed under deep surgical anaesthesia (ketaminhydrochloride 100 mg/kg and xylazinhydrochloride 5 mg/kg) at the sciatic notch. For crush injuries, the nerve was compressed for 15 seconds with fine forceps. To test early axon outgrowth ("pinch test"), mice were deeply anaesthetized 4 days after crush injury, the sciatic nerve was completely exposed and pinched with fine forceps starting from the distal end until a muscle reaction was observed. The observer was blinded regarding genotype and treatment of the mice and the regeneration distance (distance from the crush site to the pinch site where a reaction was observed) was measured with a ruler *in situ*. Footprints were acquired during the light phase by painting the hind feet of mice with black colour and letting them run along a 50 cm walking track. Prints were digitalized and the distance between toe 1 and 5 and the length of the print measured using the FOOTPRINTS program53. The sciatic functional index was calculated according to Inserra et al.,54. The observer was blinded regarding the genotype of the mice.

Electrophysiological measurements

Electrophysiological measurements were performed under deep surgical anaesthesia (ketaminhydrochloride 100 mg/kg and xylazinhydrochloride 5 mg/kg). Two recording electrodes were inserted into the intrinsic foot muscle, distal stimulation electrodes were inserted at the ankle, and proximal stimulation electrodes were inserted at the sciatic notch. Compound muscle action potentials (CMAPs) were recorded with a Jaeger-Toennies Neuroscreen instrument. Nerve conduction velocities were calculated from the distance between proximal and distal stimulation electrodes (measured *in situ*) and the latency difference between the CMAPs after successive proximal and distal stimulation. CMAP amplitudes were calculated peak to peak.

Morphology and electron microscopy

For ultrastructural analysis, nerves were immersion fixed in 2.5% glutardialdehyde and 4% paraformaldehyde in phosphate buffer and embedded into epoxy resin (Serva). Semithin sections were cut at a thickness of 0.5 μm (Leica RM 2155 using a diamond knife Histo HI 4317, Diatome) and stained with a mixture of 1% toluidine blue and 1% azur II. Ultrathin sections were cut at a thickness of 50 nm, treated with uranyl acetate and lead citrate and analysed with a Zeiss EM 900 (Leo). The g-ratio was defined as the numerical ratio between

the fiber diameter and the diameter of the same fiber including its myelin sheath and measured on electron micrographs for at least 100 randomly chosen axons per animal and nerve (3 animals per genotype and/or treatment group). Remyelinated fibers after sciatic nerve crush were counted on complete semithin cross sections of sciatic nerves (n=3 animals per genotype and/or treatment group). The percentage of myelinated and unmyelinated axons 56 days after nerve crush was quantified by counting all fibers on 25 randomly taken electron micrographs at 3000x magnification per animal (n=3 animals per genotype and treatment group). Axons per bundle were quantified on electron microscopic images by analysing all axon-Schwann cell units where the nucleus of the Schwann cell was visible (amounting to 26 randomly chosen axon-Schwann cell units per animal and nerve on average, 5 animals per genotype). For G-ratio analysis, quantification of remyelinated fibers and quantification of axons per Schwann cell, the observer was blinded regarding the genotype and/or treatment (tamoxifen or vehicle) of the animals.

Immunohistochemistry

Samples were immersion fixed using 4% phosphate buffered paraformaldehyde and embedded into paraffin wax. Immunohistochemistry was performed on 5 μm thick sections using the heat-induced antigen retrieval methods. Slides were boiled for 10 minutes in citrate buffer pH 6.0 with 0.05% Tween 20 (crushed nerves Fig. 1b) or for 20 minutes in Tris/EDTA buffer pH 9.0 with 0.05% Tween 20 (Fig. 1a) and incubated with primary antibodies over night at 4°C. The following primary antibodies were used: Zeb2 (SC27-1984, Santa Cruz: 1:200), betaIII-tubulin (TuJ1, MMS-435P, Covance 1:250), Mbp (A0623, DAKO 1:500), Krox20 (rabbit, generous gift of Dies Meijer 1:500, 55), Sox2 (SC1002, Millipore 1:200), S100β (AB52642, Abcam, 1:500, c-Jun (610327, BD Transduction). Secondary antibodies were applied for 1 hour at room temperature (Alexa Fluor® 555 donkey anti-mouse A-31570, Alexa Fluor® 488 donkey anti-mouse A-21202, Alexa Fluor® 555 donkey anti-rabbit A-31572, Alexa Fluor® 488 donkey anti-rabbit A-21206 all from Molecular Probes diluted 1:2000). For each staining, samples from at least 3 individual animals per genotype (or treatment group) were processed simultaneously and used for the analysis. Sections were examined with a Zeiss Observer fluorescence microscope or Zeiss Axiophot brightfield microscope and images acquired with ZEN2 software (Carl Zeiss Microscopy). Images were processed with Adobe Photoshop 12.0.4, Adobe Illustrator CS5 and NIH Image J 1.46R.

RNA preparation, cDNA synthesis, realtime PCR and microarray analysis—

RNA was isolated from sciatic nerves using the RNeasy Kit (Qiagen) according to manufacturer's instructions and the concentration and quality (ratio of absorption at 260/280 nm) evaluated using the NanoDrop spectrophotometer. Reverse transcription was performed with 1 μg of total RNA using the Superscript Kit (Invitrogen) and random nonamer primers. Quantitative realtime PCR was performed in triplicates for each sample using SybrGreen (Life Technologies) and the ABI PRISM 7700 detection system (Perkin Elmer). Four mice per genotype and/or treatment group were used in each experiment unless specified otherwise, relative mRNA concentrations were determined using the threshold cycle method and normalized to Rpl8. Primer sequences can be found in supplementary table 1.

Luciferase reporter assay—Promoter regions for analysis of Zeb2 binding and repression were chosen using the eukaryotic promoter database (http://epd.vital-it.ch/). The Sox2 promoter region (chromosome 3 between positions 34,648,778 - 34,650,029, mouse genome version mm10) spanned positions -1239bp to +51bp relative to the transcriptional start site of the Sox2 gene, the Hey2 promoter region (chromosome 10 between positions 30,842,764 - 30,845,280) positions -2499bp to +18bp and the Ednrb promoter region (chromosome 14 between positions 103,844,229 - 103,846,824) positions -2497bp to +99bp (variant Ednrb_1). Promoter regions were amplified by PCR and inserted as XhoI/XmaI fragments upstream of the luciferase gene into pGL2-luc (Promega). The following primers were used for PCR amplification: for Sox2 5 ´GCGCCCCGGGGGCAGGCAAGATTCTTGAAC 3´ and 5 ´GCGCCTCGAGCTCTGCCTTGACAACTCCTG 3´, for Hey2 5 ´GCGCCCCGGGCTCTGACCCAGACGTAGGAC 3´ and 5´ GCGCCTCGAGCGGCTCCTGGAGGTTCTTTC 3´ and for EdnRB 5 ´GCGCCCCGGGGGTAGTTTAATGCGCCCATC 3´ and 5 ´GCGCCTCGAGGCTGCTCCTAAACAGGCCTC 3´.

For luciferase reporter gene assays, the S16 Schwann cell line was used. Cells were transfected using polyethylenimine on 3.5 cm tissue culture plates with 1.5 μg of luciferase reporter (pGL2-luc) and varying amounts (0.3 μg, 0.9 μg or 1.5 μg) of pCMV5-Zeb2expression vector. Cells were harvested 48 h post-transfection and luciferase activity was determined in the presence of luciferin substrate by detection of chemiluminescence.

Supplementary Methods

BrdU injections and immunohistochemistry

Bromo-desoxiuridine (BrdU) was solubilized in water at a concentration of 10 mg/ml. Mice at the age of 10 or 25 days were injected intraperitoneally with one pulse of 100 μg/g body weight and sacrificed 4 hours later. Pregnant female mice at E18.5 were treated the same way and sacrificed 70 minutes after the pulse. Sciatic nerves were embedded into wax and cut at a thickness of 5 μm. For detection of BrdU-positive nuclei, sections were boiled for 10 minutes at 100 W in a microwave in citrate buffer pH6, incubated for 30 minutes at room temperature in 0.2 M glycine followed by two washes in 100 mM disodium tetraborate pH 8.5. Anti-BrdU antibody (MAB3424, Millipore) was diluted 1:200 in 2% goat serum in PBS and applied over night at 4°C. After washing, the secondary antibody (Alexa555-anti-mouse, 1:2000, A-31570, Molecular Probes) and DAPI (0.05 μg/ml) were applied for 1 hour at room temperature. For quantification of proliferating cells, all BrdU/DAPI-positive nuclei were counted on cross sections of sciatic nerves and values expressed as percentage of BrdU-positive cells relative to all DAPI-positive nuclei.

Chromatin immunoprecipitation (ChIP) assays

Pooled sciatic nerves from 15 P1 animals were dissected and immediately fixed in 1% PFA for 20 min at RT. Samples were washed once in phosphate-buffered saline, homogenized in 150 mM NaCl, 10% glycerol (vol/vol), 0.3% Triton X-100 (vol/vol) and 50 mM Tris-HCl (pH 8.0) containing protease inhibitor cocktail (Roche). Lysates were then sonicated with a

Bioruptor sonicator (Diagenode) to approx. 500 bp. Sheared chromatin was incubated with 5 μg of Zeb2 antibody (SC27-1984, Santa Cruz) ON 4°C. ChIP was performed using the The Magna ChIP G Kit (Merck Millipore) according to manufacturer's instructions. Quantitative realtime PCR was performed using SybrGreen (Life Technologies) and the ABI PRISM 7700 detection system (Perkin Elmer). The relative fold enrichments were determined by the $2^{-\Delta CT}$ method and samples were normalized to input chromatin. Primers used for PCR analysis are provied in Suppl. table 1.

Data availability

The primary data that support the findings of this study are available from the coresponding authors upon request.

Supplementary Material

Refer to Web version on PubMed Central for supplementary material.

Acknowledgments

The authors would like to thank C. Maack, T. Durkaya and A. Fahrenholz for excellent technical assistance. We thank the staff of the Transcriptome Analysis Laboratory (TAL) of the University Medical Center Göttingen for performance and statistical analysis of the microarray analysis and A. Diedrich, M. Wehe, B. Nickel and T. Hoffmeister for excellent support in animal husbandry. We are grateful to Dr. Q. Richard Lu for communicating unpublished data. The DH lab was supported by Belspo-IAP funding (IAPVII-07), FWO-V (G.0782.14), Hercules Foundation (ZW09-03 project InfraMouse) and Erasmus MC start-up funds. M.W.S. is supported by a Heisenberg Professorship granted by the DFG (GZ: SE 1944/1-1). K.-A.N. is supported by the DFG (Research Center Molecular Physiology of the Brain, CNMPB) and holds a European Research Council Advanced Investigator Grant (ERC_269020).

References

1. Jessen KR, Mirsky R. Negative regulation of myelination: Relevance for development, injury, and demyelinating disease. Glia. 2008; 56:1552–1565. [PubMed: 18803323]
2. Monk KR, Feltri ML, Taveggia C. New insights on schwann cell development. Glia. 2015; 63:1376–1393. [PubMed: 25921593]
3. Stolt CC, Wegner M. Schwann cells and their transcriptional network: Evolution of key regulatorsof peripheral myelination. Brain Research. 2015; :1–10. DOI: 10.1016/j.brainres.2015.09.025
4. Topilko P, et al. Krox-20 controls myelination in the peripheral nervous system. Nature. 1994; 371:796–799. [PubMed: 7935840]
5. Decker L. Peripheral Myelin Maintenance Is a Dynamic Process Requiring Constant Krox20 Expression. Journal of Neuroscience. 2006; 26:9771–9779. [PubMed: 16988048]
6. Ghislain J, Charnay P. Control of myelination in Schwann cells: a Krox20 cis-regulatory element integrates Oct6, Brn2 and Sox10 activities. EMBO Rep. 2006; 7:52–58. [PubMed: 16311519]
7. Kuhlbrodt K, Herbarth B, Sock E, Hermans-Borgmeyer I, Wegner M. Sox10, a novel transcriptional modulator in glial cells. J Neurosci. 1998; 18:237–250. [PubMed: 9412504]
8. Britsch S. The transcription factor Sox10 is a key regulator of peripheral glial development. Genes & Development. 2001; 15:66–78. [PubMed: 11156606]
9. Finzsch M, et al. Sox10 is required for Schwann cell identity and progression beyond the immature Schwann cell stage. The Journal of Cell Biology. 2010; 189:701–712. [PubMed: 20457761]
10. Fröb F, et al. Establishment of myelinating schwann cells and barrier integrity between central and peripheral nervous systems depend on Sox10. Glia. 2012; 60:806–819. [PubMed: 22337526]
11. Bremer M, et al. Sox10 is required for Schwann-cell homeostasis and myelin maintenance in the adult peripheral nerve. Glia. 2011; 59:1022–1032. [PubMed: 21491499]

12. Le N, et al. Nab proteins are essential for peripheral nervous system myelination. Nature Neuroscience. 2005; 8:932–940. [PubMed: 16136673]
13. Desmazieres A, Decker L, Vallat JM, Charnay P, Gilardi-Hebenstreit P. Disruption of Krox20-Nab Interaction in the Mouse Leads to Peripheral Neuropathy with Biphasic Evolution. Journal of Neuroscience. 2008; 28:5891–5900. [PubMed: 18524893]
14. Mager GM, et al. Active Gene Repression by the Egr2{middle dot}NAB Complex during Peripheral Nerve Myelination. Journal of Biological Chemistry. 2008; 283:18187–18197. [PubMed: 18456662]
15. He Y, et al. The transcription factor Yin Yang 1 is essential for oligodendrocyte progenitor differentiation. Neuron. 2007; 55(2):217–30. [PubMed: 17640524]
16. He Y, et al. Yy1 as a molecular link between neuregulin and transcriptional modulation of peripheral myelination. Nature Neuroscience. 2010; 13:1472–1480. [PubMed: 21057508]
17. Verschueren K, et al. SIP1, a Novel Zinc Finger/Homeodomain Repressor, Interacts with Smad Proteins and Binds to 5'-CACCT Sequences in Candidate Target Genes. Journal of Biological Chemistry. 1999; 274:20489–20498. [PubMed: 10400677]
18. Conidi A, et al. Few Smad proteins and many Smad-interacting proteins yield multiple functions and action modes in TGFbeta/BMP signalling in vivo. Cytokine and Growth Factor Reviews. 2011; 22:287–300. [PubMed: 22119658]
19. Comijn J, et al. The two-handed E box binding zinc finger protein SIP1 downregulates E-cadherin and induces invasion. Mol Cell. 2001; 7:1267–1278. [PubMed: 11430829]
20. Vandewalle C. SIP1/ZEB2 induces EMT by repressing genes of different epithelial cell-cell junctions. Nucleic Acids Research. 2005; 33:6566–6578. [PubMed: 16314317]
21. Dai Y-H, et al. ZEB2 Promotes the Metastasis of Gastric Cancer and Modulates Epithelial Mesenchymal Transition of Gastric Cancer Cells. Dig Dis Sci. 2012; 57:1253–1260. [PubMed: 22350782]
22. Seuntjens E, et al. Sip1 regulates sequential fate decisions by feedback signaling from postmitotic neurons to progenitors. Nature Neuroscience. 2009; 12:1373–1380. [PubMed: 19838179]
23. Weng Q, et al. Dual-Mode Modulation of Smad Signalingby Smad-Interacting Protein Sip1 Is Required for Myelination in the Central Nervous System. Neuron. 2012; 73:713–728. [PubMed: 22365546]
24. Van de Putte T, Francis A, Nelles L, van Grunsven LA, Huylebroeck D. Neural crest-specific removal of Zfhx1b in mouse leads to a wide range of neurocristopathies reminiscent of Mowat-Wilson syndrome. Human Molecular Genetics. 2007; 16:1423–1436. [PubMed: 17478475]
25. Mowat DR, et al. Hirschsprung disease, microcephaly, mental retardation, and characteristic facial features: delineation of a new syndrome and identification of a locus at chromosome 2q22-q23. J Med Genet. 1998; 35:617–623. [PubMed: 9719364]
26. Stanchina L, Van de Putte T, Goossens M, Huylebroeck D, Bondurand N. Developmental Biology. Genetic interaction between Sox10 an Zfhx1b during enteric nervous sstem development. Developmental Biology. 2010; 341:416–428. [PubMed: 20206619]
27. Higashi Y, et al. Generation of the floxed allele of the SIP1 (Smad-interacting protein 1) gene for Cre-mediated conditional knockout in the mouse. genesis. 2002; 32:82–84. [PubMed: 11857784]
28. Jaegle M. The POU proteins Brn-2 and Oct-6 share important functions in Schwann cell development. Genes & Development. 2003; 17:1380–1391. [PubMed: 12782656]
29. Jessen KR, Mirsky R. The origin and development of glial cells in peripheral nerves. Nat Rev Neurosci. 2005; 6:671–682. [PubMed: 16136171]
30. Colognato H, Tzvetanova ID. Glia unglued: How signals from the extracellular matrix regulate the development of myelinating glia. Devel Neurobio. 2011; 71:924–955.
31. Brennan A, et al. Endothelins control the timing of Schwann cell generation in vitro and in vivo. Developmental Biology. 2000; 227:545–557. [PubMed: 11071773]
32. Druckenbrod NR, Powers PA, Bartley CR, Walker JW, Epstein ML. Targeting of endothelin receptor-B to the neural crest. genesis. 2008; 46:396–400. [PubMed: 18693272]
33. Xin M, et al. Essential roles of the bHLH transcription factor Hrt2 in repression of atrial gene expression and maintenance of postnatal cardiac function. Proc Natl Acad Sci USA. 2007; 104:7975–7980. [PubMed: 17468400]

34. Leone DP, et al. Tamoxifen-inducible glia-specific Cre mice for somatic mutagenesis in oligodendrocytes and Schwann cells. Molecular and Cellular Neuroscience. 2003; 22:430–440. [PubMed: 12727441]
35. Madisen L, et al. A robust a high-thhroughput Cre reporting and characterization system for the whole mouse brain. Nature Neuroscience. 2009; 13:133–140. [PubMed: 20023653]
36. Wu LMN, et al. Zeb2 recruits HDAC-NuRD to Inhibit Notch and Controls Schwann Cell Differentiation and Remyelination. Nature Neuroscience. 2016
37. Weider M, et al. Short Article. Chromatin-remodelling factor Brg1 is required for Schwann cell differentiation and myelination. Developmental Cell. 2012; 23:193–201. [PubMed: 22814607]
38. Bermingham JR, et al. Tst-1/Oct-6/SCIP regulates a unique step in peripheral myelination and is required for normal respiration. Genes & Development. 1996; 10:1751–1762. [PubMed: 8698235]
39. Jaegle M, et al. The POU factor Oct-6 and Schwann cell differentiation. Science. 1996; 273:507–510. [PubMed: 8662541]
40. Verstappen G, et al. Atypical Mowat-Wilson patient confirms the importance of the novel association between ZFHX1B/SIP1 and NuRD corepressor complex. Human Molecular Genetics. 2008; 17:1175–1183. [PubMed: 18182442]
41. Berti C, et al. Non-redundant function of dystroglycan and 1 integrins in radial sorting of axons. Development. 2011; 138:4025–4037. [PubMed: 21862561]
42. Yang D. Coordinate control of axon defasciculation and myelination by laminin-2 and -8. The Journal of Cell Biology. 2005; 168:655–666. [PubMed: 15699217]
43. Le N, et al. Analysis of congenital hypomyelinating Egr2Lo/Lo nerves identifies Sox2 as an inhibitor of Schwann cell differentiation and myelination. Proc Natl Acad Sci USA. 2005; 102:2596–2601. [PubMed: 15695336]
44. Weber D, et al. Journal of Molecular and Cellular Cardiology. Journal of Molecular and Cellular Cardiology. 2015; 79:79–88. [PubMed: 25446183]
45. Woodhoo A, et al. Notch controls embryonic Schwann cell differentiation, postnatal myelination and adult plasticity. Nature Neuroscience. 2009; 12:839–847. [PubMed: 19525946]
46. Evans E, et al. The behavioral phenotype of Mowat-Wilson syndrome. Am J Med Genet. 2012; 158A:358–366. [PubMed: 22246645]
47. Pradier B, et al. Smad-interacting protein 1 affects acute and tonic, but not chronic pain. EJP. 2013; 18:249–257. [PubMed: 23861142]
48. Emery B. Regulation of oligodendrocyte differentiation and myelination. Science. 2010; 330:779–782. [PubMed: 21051629]
49. Li H, He Y, Richardson WD, Casaccia P. Two-tier transcriptional control of oligodendrocyte differentiation. Current Opinion in Neurobiology. 2009; 19:479–485. [PubMed: 19740649]
50. Arthur-Farraj PJ, et al. c-Jun reprograms Schwann cells of injured nerves to generate a repair cell essential for regeneration. Neuron. 2012; 75:633–647. [PubMed: 22920255]
51. Adameyko I, et al. Schwann Cell Precursors from Nerve Innervation Are a Cellular Originof Melanocytes in Skin. Cell. 2009; 139:366–379. [PubMed: 19837037]
52. Toda K, Small JA, Goda S, Quarles RH. Biochemical and cellular properties of three immortalized Schwann cell lines expressing different levels of the myelin-associated glycoprotein. Journal of Neurochemistry. 1994; 63:1646–1657. [PubMed: 7523597]
53. Klapdor K, Dulfer BG, Hammann A, Van der Staay FJ. A low-cost method to analyse footprint patterns. Journal of Neuroscience Methods. 1997; 75:49–54. [PubMed: 9262143]
54. Inserra MM, Bloch DA, Terris DJ. Functional indices for sciatic, peroneal, and posterior tibial nerve lesions in the mouse. Microsurgery. 1998; 18:119–124. [PubMed: 9674927]
55. Darbas A, et al. Cell autonomy of the mouse claw paw mutation. Developmental Biology. 2004; 272:470–482. [PubMed: 15282162]

Europe PMC Funders Author Manuscripts

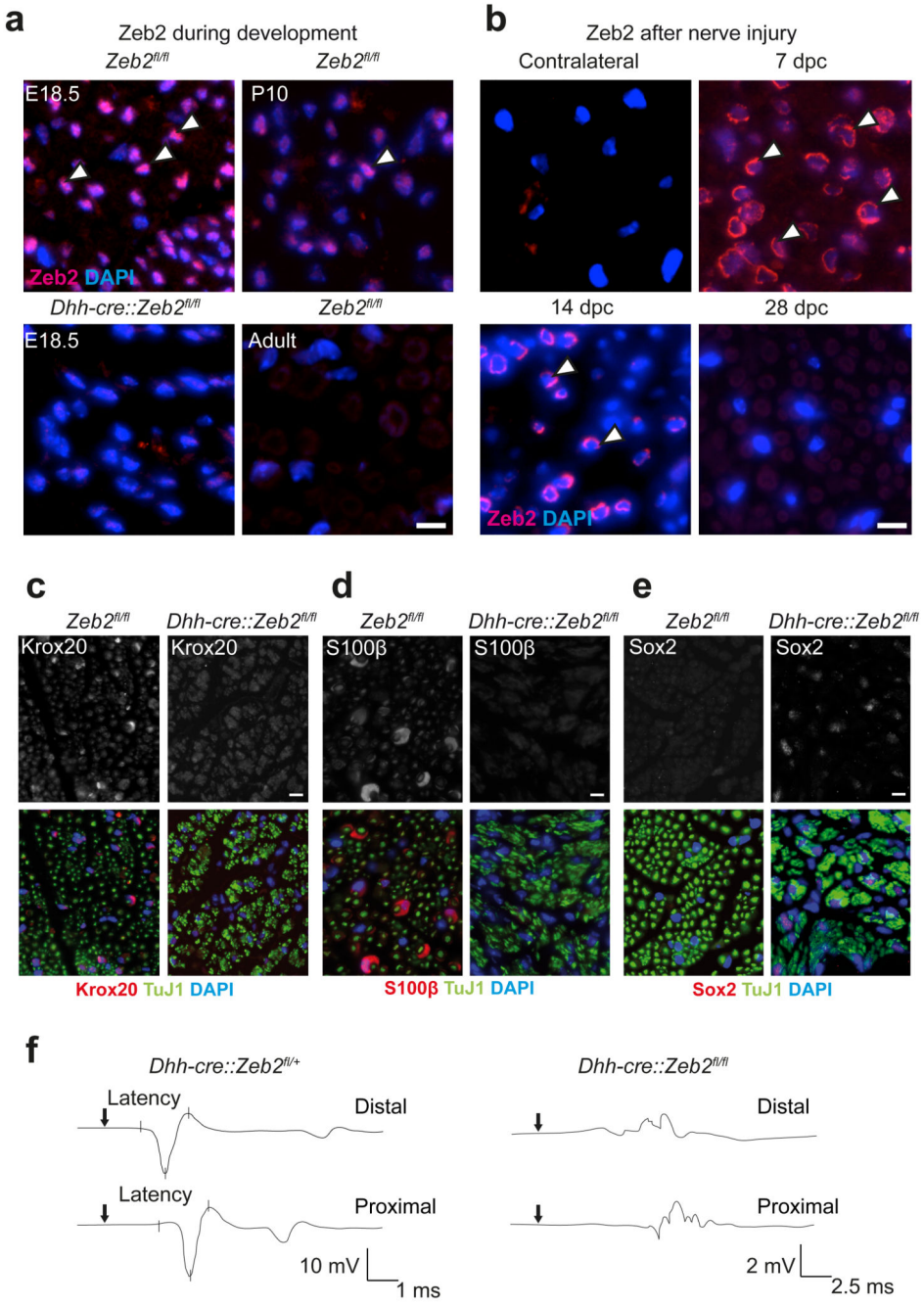

Figure 1. Functional analysis of Zeb2 in Schwann cell development and nerve repair.

(a) Nuclear Zeb2 immunofluorescence (pink, white arrow heads) of sciatic nerve cross sections at different developmental stages. Zeb2 is absent from Schwann cells of *Dhh-cre::Zeb2*$^{fl/fl}$ mice at age E18.5 (lower left). Representative images of n=3 animals per time point and genotype. Scale bars, 10 μm.

(b) Zeb2 reexpression at different time points after nerve crush in the distal stump of sciatic nerves (pink, white arrow heads, dpc: days post crush, contralateral: unharmed nerve). Representative images of n=3 animals per time point and genotype. Scale bars, 10 μm.

(c)-(e) Immunohistochemistry of sciatic nerve cross sections from *Dhh-cre::Zeb2*$^{fl/fl}$ mice and controls at P25 comparing Krox20 (in c), S100β (in d) and Sox2 (in e), all in red/white (top). Axons, green (TuJ1). Schwann cell nuclei, blue (DAPI). Representative images of n=3 animals per genotype. Scale bars, 10 μm. Experiments in panels **a-e** were successfully repeated in 3 animals per genotype and time point.

(f) Electrophysiological recording of CMAPs with proximally and distally stimulated sciatic nerves from *Dhh-cre::Zeb2*$^{fl/+}$ (left) and *Dhh-cre::Zeb2*$^{fl/fl}$ mice (right) at age P25. Representative traces from measurements of 3 individual mice per genotype are shown.

Europe PMC Funders Author Manuscripts

Europe PMC Funders Author Manuscripts

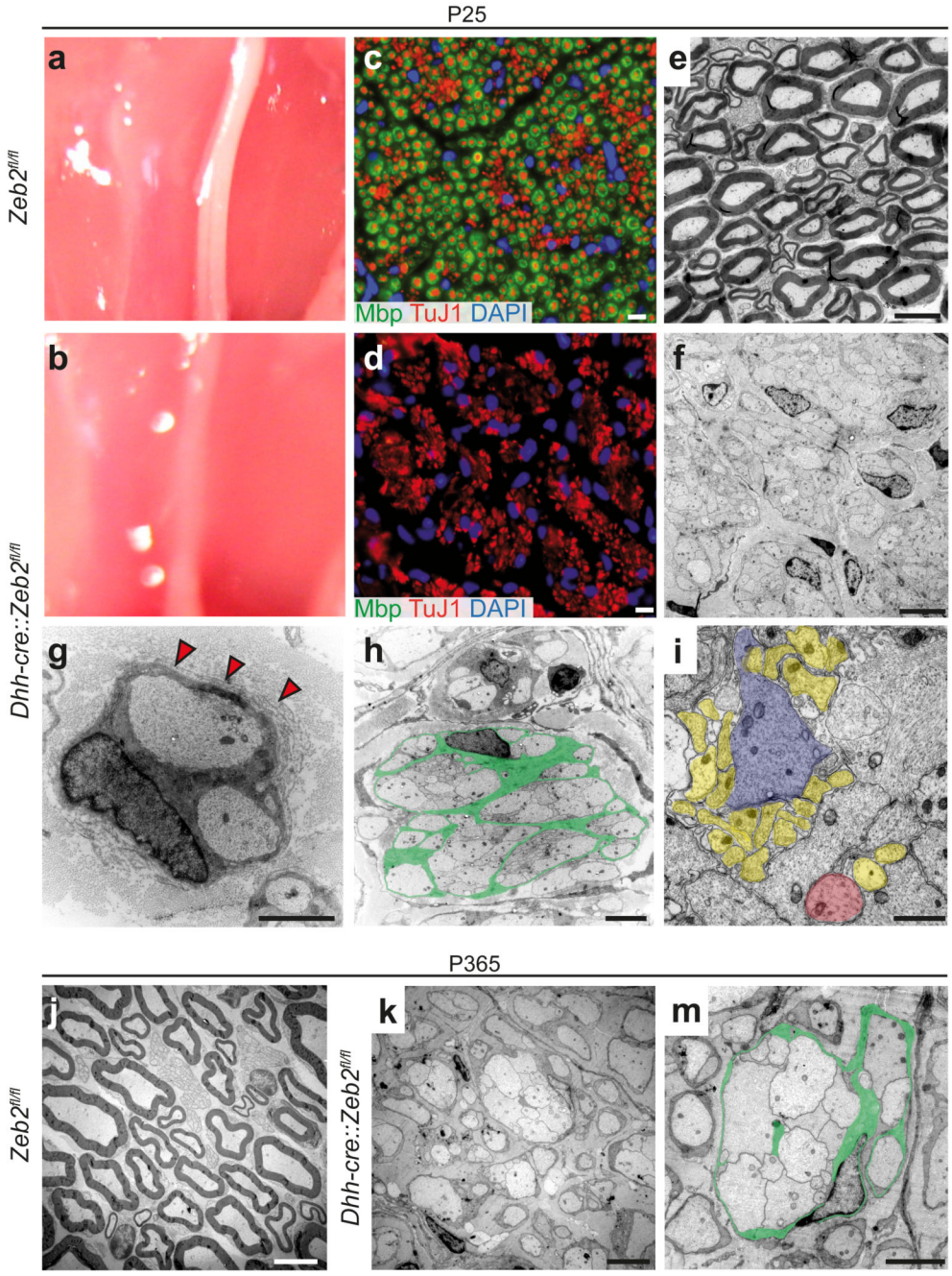

Figure 2. Mice lacking Zeb2 in Schwann cells develop severe neuropathy.

(a, b) Compared to control sciatic nerves at age P25, *Dhh-cre::Zeb2*$^{fl/fl}$ mutant nerves are translucent.

(c, d) By immunostaining, MBP-stained myelin (in green) surrounds TuJ1 stained axons (in red). Note the absence of myelin in **(d)**. DAPI, Schwann cell nuclei. Scale bars, 10 μm. The experiment was successfully repeated in 3 animals per genotype and representative images are shown.

(e, f) By electron microscopy, mutant nerves are amyelinated (in f). Scale bars, 2.5 μm.

(g) Zeb2-deficient Schwann cell arrested in sorting with two engulfed axons and supernumerary loops of basal lamina (red arrow heads). Scale bar, 1 μm.
(h) Mutant Schwann cell (cytoplasm false-coloured in green) surrounding without sorting>50 axons. Scale bar, 1 μm.
(i) Bundle of unsorted axons that differ in size as indicated by false colours (yellow, small sized; red: medium sized; purple: large sized). Scale bar, 1 μm.
(j-m) At one year of age, conditional mutants showed persistent lack of sorting and amyelination (in k, m). Green: Schwann cell cytoplasm false coloured. Axons appear intact. Scale bars, 2.5 μm. All electron micrographs shown in panels **e-m** are representative of 3 mice per genotype and age.

Europe PMC Funders Author Manuscripts

Europe PMC Funders Author Manuscripts

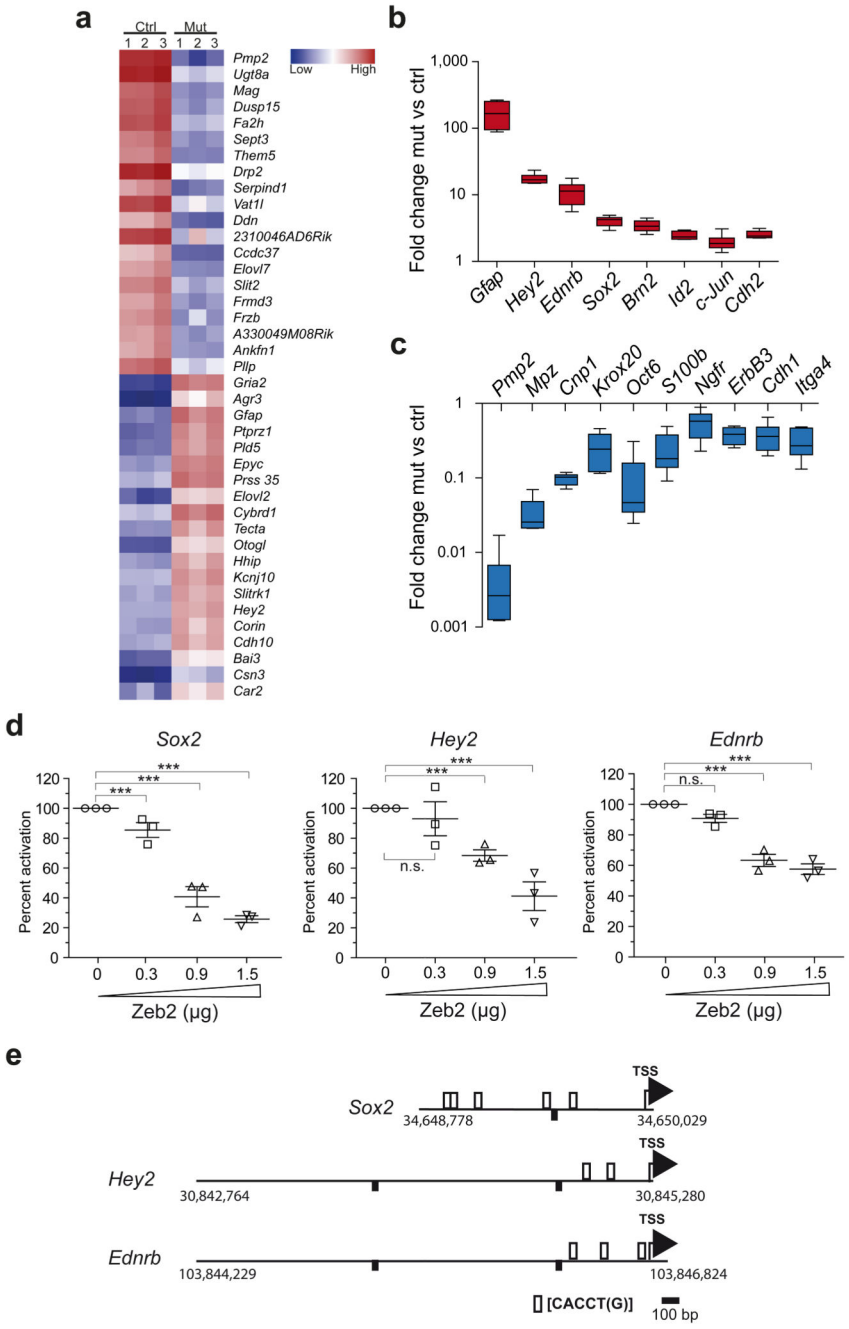

Figure 3. Zeb2-deficient Schwann cells continuously express developmental inhibitors.

(a) Heat map of a microarray analysis depicting the 20 most up-and downregulated genes in sciatic nerves of 3 *Dhh-cre::Zeb2*$^{fl/fl}$ mice (Mut) compared to littermate controls (Ctrl) at age P25.

(b, c) A subset of promyelinating factors and developmental inhibitors was confirmed by quantitative realtime PCR. Note the logarithmic scale. Statistics, n=6 animals per genotype, except for GFAP n=3 mutants and 4 controls, two-sided student's t-test of unpaired samples. P-values: Gfap P=0.026, t=3.461, Hey2 P=4.57E-05, t=12.67411, Ednrb P=0.002, t=5.740,

Sox2 P=1.4E-05, t=8.247414, Brn2 P=0.0006, t=4.939481, Id2 P=0.0004, t=5.430061, c-Jun P=0.008, t=4.013638, Cdh2 P=8.18E-06, t=8,972395, Pmp2 P=3.5E-05, t=13.80419, Mpz P=0.0001, t=9.639648, Cnp1 P=9.56E-05, t=11.06300, Krox20 P=0.002, t=4.786690, Oct6 P=0.001, t=6.015117, S100β P=0.002, t=4.855561, Ngfr P=0.005, t=3.579138, ErbB3 P=0.0003, t=6.287818, Cdh1 P=0.0006, t=5.291520, Itga4 P=0.0003, t=6.020152. Whiskers show the minimum and maximum, boxes extend from the first to the third quartiles with cross lines at the median.

(d) Luciferase assays revealing *Zeb2* gene dosage-dependent reduction of promoter activity of *Sox2*, *Hey2*, and *Ednrb* in S16 cells upon cotransfection with a Zeb2 expression plasmid. Each dot represents 1 independent experiment with 3 replicates ±SEM with cross lines at the mean. Activity of lysates from cells co-transfected with the plasmid containing the respective promoter fragment and the empty pCMV5 plasmid was considered 100%. (n=3 independent experiments with 3 replicates, One-sided student's t-test of unpaired samples Ednrb: P=0.091, t=1.392353, P=2.48E-05, t=5.488391, P=2.6E-06, t=6.688200; Hey2: P=0.162, t=1.016833, P=2.88E-06, t=6.631628, P=2.16E-08, t=9.678931; Sox2: P=0.0005, t=3.977938, P=2.89E-11, t=15.28166, P=1.46E-14, t=25.04342, n.s. not significant).

(e) Promoter fragments with murine genomic localization and predicted Zeb2 binding sites (as used in **d**).

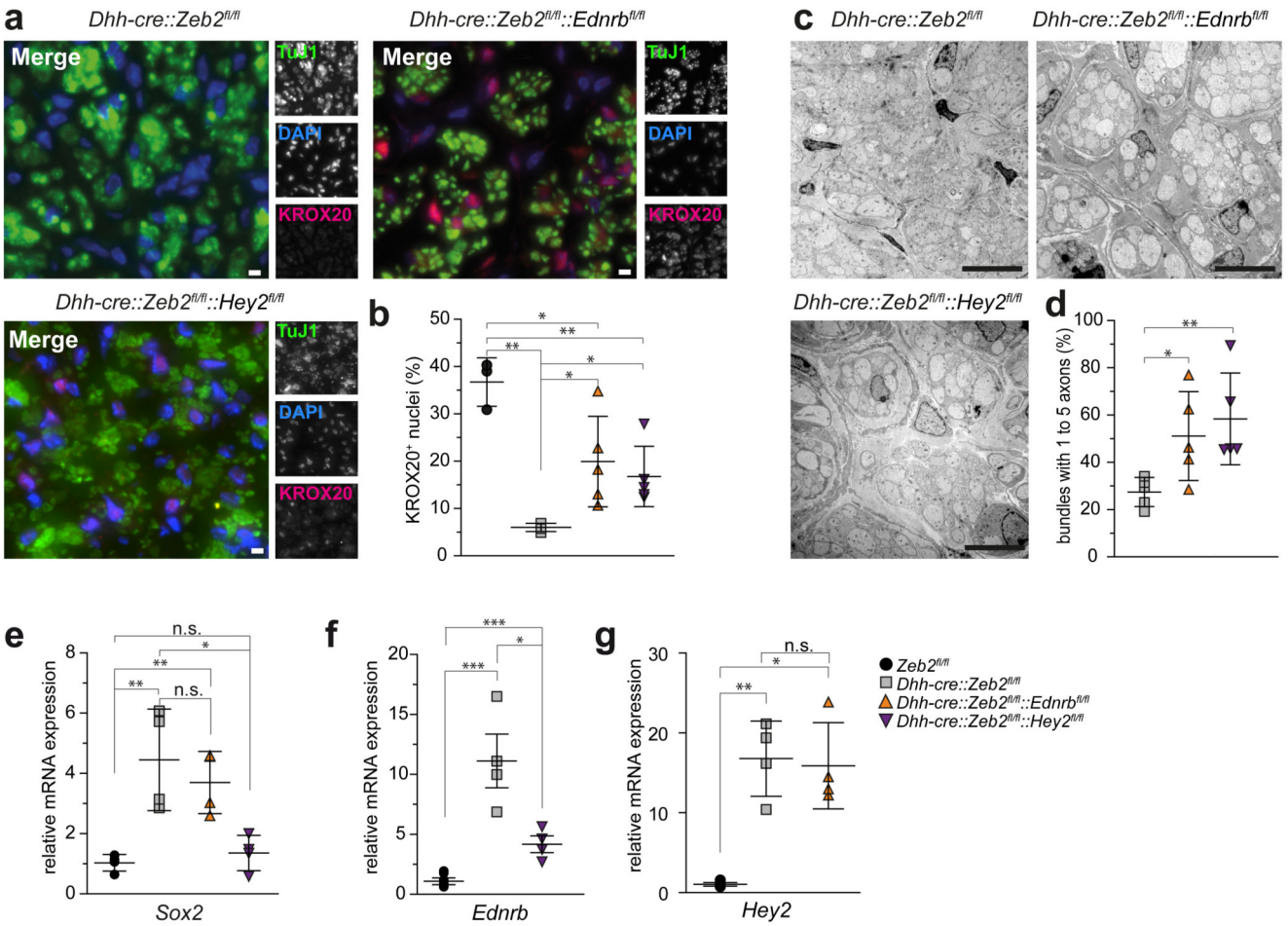

Figure 4. Zeb2-mediated repression of *Ednrb* and *Hey2* is functionally relevant.

(a) Virtual absence of Krox20 from Zeb2 cKO Schwann cells (upper left) and reemergence in a subpopulation of Schwann cells in both *Zeb2/Ednrb* (upper right) and *Zeb2/Hey2* conditional double mutant mice (lower left). Green: axons (TuJ1). Blue: Schwann cell nuclei (DAPI). Red: Krox20. Scale bars, 5 μm. The experiment was successfully repeated with sections from 5 animals per genotype (except $Zeb2^{fl/fl}$ n=3 and $Dhh\text{-}cre::Zeb2^{fl/fl}$ n=4) and representative images are shown.

(b) Quantification of the Krox20-positive nuclei shown in **(a).** Each dot represents one individual animal ±SD with cross lines at the mean. Statistics: n=5 animals per genotype (except $Zeb2^{fl/fl}$ n=3 and $Dhh\text{-}cre::Zeb2^{fl/fl}$ n=4). Significance: $Zeb2^{fl/fl}$ vs. $Dhh\text{-}cre::Zeb2^{fl/fl}$ P=0.008, t=12.17175, $Dhh\text{-}cre::Zeb2^{fl/fl}$vs. $Dhh\text{-}cre::Zeb2^{fl/fl}::Ednrb^{fl/fl}$ P=0.03, t=2.858292, $Dhh\text{-}cre::Zeb2^{fl/fl}$ vs. $Dhh\text{-}cre::Zeb2^{fl/fl}::Hey2^{fl/fl}$ P=0.013, t=3.299356, $Zeb2^{fl/fl}$ vs. $Dhh\text{-}cre::Zeb2^{fl/fl}::Hey2^{fl/fl}$ P=0.004, t=4.564169, $Zeb2^{fl/fl}$ vs. $Dhh\text{-}cre::Zeb2^{fl/fl}::Ednrb^{fl/fl}$ P=0.03, t=2.760013 (two-sided student's t-test of unpaired samples, * P <0.05; ** P <0.01; *** P <0.001).

(c) Improved radial sorting and smaller axon bundles in sciatic nerves of conditional *Zeb2/Ednrb* (upper right) and *Zeb2/Hey2* (lower left) double mutant mice compared to conditional

Europe PMC Funders Author Manuscripts

Zeb2 single mutants (upper left) at age P25. Scale bars, 5 μm. Representative images of 5 mice per genotype.

(d) Higher number of bundles with only 1 to 5 axons per Schwann cell in both double mutant mice at age P25 compared to *Zeb2* single mutants. Statistics: n=5 animals per genotype (on average 26 randomly chosen bundles per animal, each dot represents the mean percentage of bundles from one individual animal ±SD with cross lines at the mean). *Dhh-cre::Zeb2*$^{fl/fl}$ vs. *Dhh-cre::Zeb2*$^{fl/fl}$*::Ednrb*$^{fl/fl}$ P=0.0283, t=2.670897, *Dhh-cre::Zeb2*$^{fl/fl}$ vs. *Dhh-cre::Zeb2*$^{fl/fl}$*::Hey2*$^{fl/fl}$ P=0.0031, t=4.185530 (Two-sided student's t-test of unpaired samples, * P <0.05; ** P <0.01).

(e) Sox2 expression at age P25 was significantly upregulated in *Dhh-cre::Zeb2*$^{fl/fl}$ mice and *Dhh-cre::Zeb2*$^{fl/fl}$*::Ednrb*$^{fl/fl}$ mice, but not in *Dhh-cre::Zeb2*$^{fl/fl}$*::Hey2*$^{fl/fl}$ mice compared to *Zeb2*$^{fl/fl}$ mice. Significance: *Zeb2*$^{fl/fl}$ vs. *Dhh-cre::Zeb2*$^{fl/fl}$ P=0.0071, t=3.999399, *Dhh-cre::Zeb2*$^{fl/fl}$ vs. *Dhh-cre::Zeb2*$^{fl/fl}$*::Ednrb*$^{fl/fl}$ P=0.480, t=0.7625912, *Dhh-cre::Zeb2*$^{fl/fl}$ vs. *Dhh-cre::Zeb2*$^{fl/fl}$*::Hey2*$^{fl/fl}$ P=0.0133, t=3.467755, *Zeb2*$^{fl/fl}$ vs. *Dhh-cre::Zeb2*$^{fl/fl}$*::Hey2*$^{fl/fl}$ P=0.3598, t=0.9913170, *Zeb2*$^{fl/fl}$ vs. *Dhh-cre::Zeb2*$^{fl/fl}$*::Ednrb*$^{fl/fl}$ P=0.0025, t=4.978021 (n=4 mice per genotype, two-sided Student's t-test of unpaired samples, * P <0.05; ** P <0.01, n.s. not significant).

(f) Ednrb expression at age P25 was significantly upregulated in *Dhh-cre::Zeb2*$^{fl/fl}$ mice and *Dhh-cre::Zeb2*$^{fl/fl}$*::Hey2*$^{fl/fl}$ mice compared to controls (n=4 *Zeb2*$^{fl/fl}$ mice and 4 *Zeb2*$^{fl/fl}$*::Hey2*$^{fl/fl}$ mice). Expression in *Dhh-cre::Zeb2*$^{fl/fl}$*::Hey2*$^{fl/fl}$ mice was significantly lower than in *DhhCre::Zeb2*$^{fl/fl}$ mice (n=4 mice per genotype: controls vs. *Dhh-cre::Zeb2*$^{fl/fl}$ P=2.5588E-5, t=7.314075, *Dhh-cre::Zeb2*$^{fl/fl}$ vs. *Dhh-cre::Zeb2*$^{fl/fl}$*::Hey2*$^{fl/fl}$ P=0.0163, t=3.303197, controls vs. *Dhh-cre::Zeb2*$^{fl/fl}$*::Hey2*$^{fl/fl}$ P=9.4176E-5, t=6.257124, two-sided Student's t-test of unpaired samples, * P <0.05; *** P <0.001).

(g) Hey2 expression at age P25 was significantly higher in *Dhh-cre::Zeb2*$^{fl/fl}$*::Ednrb*$^{fl/fl}$ mice compared to controls (n=4 *Zeb2*$^{fl/fl}$ mice and 4 *Zeb2*$^{fl/fl}$*::Ednrb*$^{fl/fl}$ mice). and not significantly different from *Dhh-cre::Zeb2*$^{fl/fl}$ mice. Significance: controls vs. *Dhh-cre::Zeb2*$^{fl/fl}$ P=0.00676, t=9.932308, *Dhh-cre::Zeb2*$^{fl/fl}$ vs. *Dhh-cre::Zeb2*$^{fl/fl}$*::Ednrb*$^{fl/fl}$ P=0.8133, t=0.2467216, controls vs. *Dhh-cre::Zeb2*$^{fl/fl}$*::Ednrb*$^{fl/fl}$ P=0.047, t=8.177906 (n=4 mice per genotype, two-sided student's t-test of unpaired samples, * P <0.05; ** P <0.01, n.s. not significant).

Europe PMC Funders Author Manuscripts

Europe PMC Funders Author Manuscripts

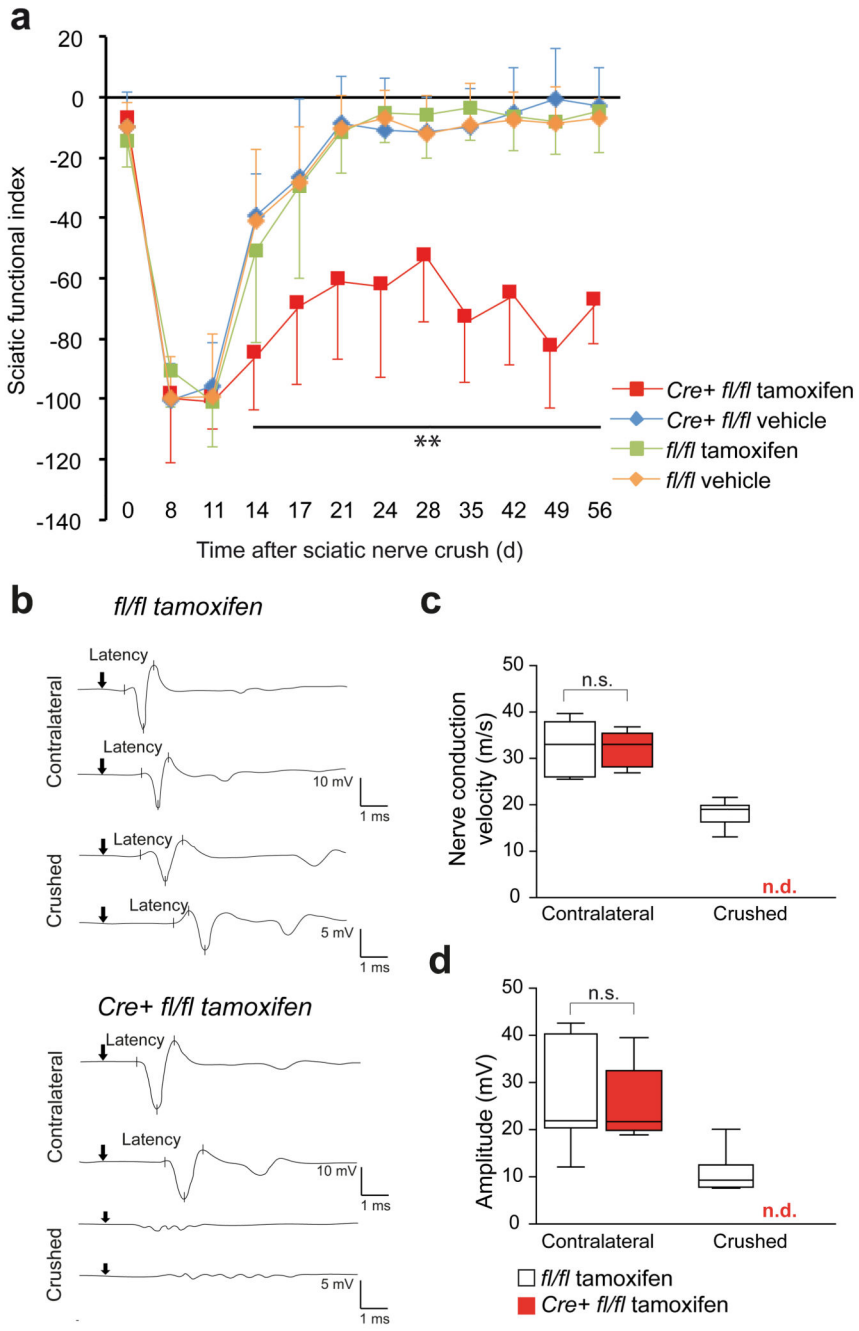

Figure 5. Zeb2 is required for efficient recovery after nerve injury.

(a) Functional recovery after nerve crush is significantly perturbed in tamoxifen-treated *PLP-creERT2::Zeb2*$^{fl/fl}$ mice (Cre+ fl/fl tamoxifen, in red) in comparison to 3 control groups, as determined by the sciatic functional index. Dots depict mean ±SD, n=a minimum of 10 animals per group. (one-way ANOVA day 0: P=0.3064, F(3,38)=1.246703, day 8: P=0.3577, F(3,39)=1.107561, day 11 P=0.8386, F(3,44)=0.2813102, day 14 P=0.0001, F (3,39)=8.903, day 17 P=0.0001, F(3,45)=8.481348, day 21 P=4.23781E-10, F(3,46)=26.47369, day 24, P=1.52347E-8, F(3,37)=22.85789, day 28, P=6.29699E-9,

F(3,41)=23.14702, day 35 P=3.00629E-14, F(3,40)=54.95588, day 42, P=5.11929E-12, F(3,41)=38.61261, day 49, P=4.01117E-16, F(3,40)=71.49940, day 56 P=7.98803E-15, F(3,39)=61.31167.

(b) Electrophysiological recordings of CMAPs after sciatic nerve stimulation 52 days after crush injury. Note the persistent conduction blocks in tamoxifen-treated *PLP-creERT2::Zeb2*$^{fl/fl}$mice (bottom) in contrast to control nerves that had regained functional nerve conduction. Representative traces of 8 *Zeb2*$^{fl/fl}$ tamoxifen-treated mice and 5 *PLP-creERT2::Zeb2*$^{fl/fl}$ tamoxifen-treated mice are shown.

(c) Nerve conduction velocity was regained to about 54% in control nerves but could not be determined (n.d.) in conditional *Zeb2* mutants. Whiskers show the minimum and maximum, boxes extend from the first to the third quartiles with cross lines at the median. (*Zeb2*$^{fl/fl}$ tamoxifen-treated: n=7 animals, *PLP-creERT2::Zeb2*$^{fl/fl}$ animals tamoxifen-treated: n=5, two-sided student's t-test of unpaired samples P=0.8737, t=0.16361498, n.s. not significant).

(d) CMAP amplitudes as a measure of functional renervation were partly restored in control mice but remained undetectable (n.d.) in conditional *Zeb2* mutants. Whiskers show the minimum and maximum, boxes extend from the first to the third quartiles with cross lines at the median. (*Zeb2*$^{fl/fl}$ tamoxifen-treated: n=7 animals, *PLP-creERT2::Zeb2*$^{fl/fl}$ animals tamoxifen-treated: n=5, two-sided student's t-test of unpaired samples P=0.9022, t=0.1260085, n.s. not significant).

Europe PMC Funders Author Manuscripts

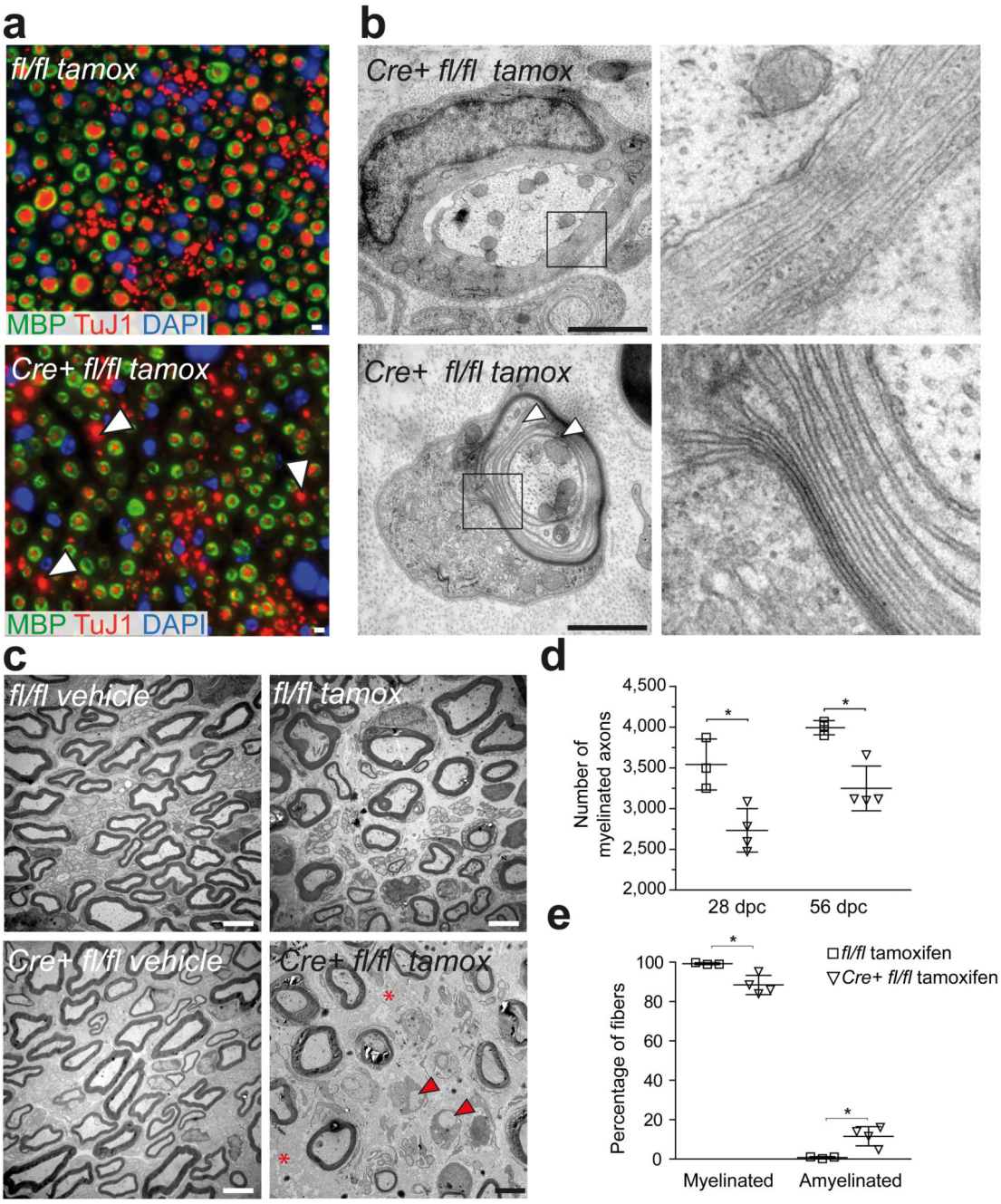

Figure 6. Remyelination by Zeb2-deficient Schwann cells is impaired

(a) In contrast to control mice, 56 days after sciatic nerve crush injury (top), tamoxifen-treated *PLP-creERT2::Zeb2*$^{fl/fl}$ mice (bottom) have many amyelinated fibers remaining (white arrow heads), as visualized by costaining axons (TuJ1, red) and myelin sheaths (MBP, green). The experiment was successfully repeated with sections from 3 animals per group and representative images (see also quantification in d) are shown. Scale bars, 5 μm.

Europe PMC Funders Author Manuscripts

(b) By electron microscopy 56 days after nerve crush, mutant mice still exhibit signs of ongoing remyelination, such as cytoplasm-filled myelin wraps (top) and thinly compact sheaths (bottom). Boxed areas are magnified to the right. Scale bars, 1 μm.
(c) In contrast to various controls that regenerate well, tamoxifen-treated *PLP-creERT2::Zeb2*$^{fl/fl}$ mice (bottom right) exhibit axon-free fibrotic areas (red asterisks) and unmyelinated axons (red arrow heads). Scale bars, 2.5 μm. Electron micrographs in panels b and c are representative of 4 animals per treatment and genotype.
(d) Impaired axonal regeneration and remyelination in mutant mice. Note that fewer myelinated axons (>1 μm) are seen 28 and 56 days after sciatic nerve crush on semi-thin sections. Each dot represents 1 individual mouse ±SD (*Zeb2*$^{fl/fl}$ tamoxifen-treated: n=3, *PLP-creERT2::Zeb2*$^{fl/fl}$ tamoxifen-treated: n=4, two-tailed student's t-test of unpaired samples, 28 days: P=0.014, t=3.697461, 56 days: P=0.0063, t=4.520971 * P <0.05).
(e) Confirmation at the EM level (56 dpc), where amyelinated axons can be clearly visualized (same animals as in d). Each dot represents 1 individual mouse ±SD (25 randomly chosen electron micrographs at 3000x magnification per animal, amyelinated P=0.0137, t=3.721040 myelinated P=0.0137, t=3.721040, two-tailed student's t-test of unpaired samples, * P <0.05).

Europe PMC Funders Author Manuscripts

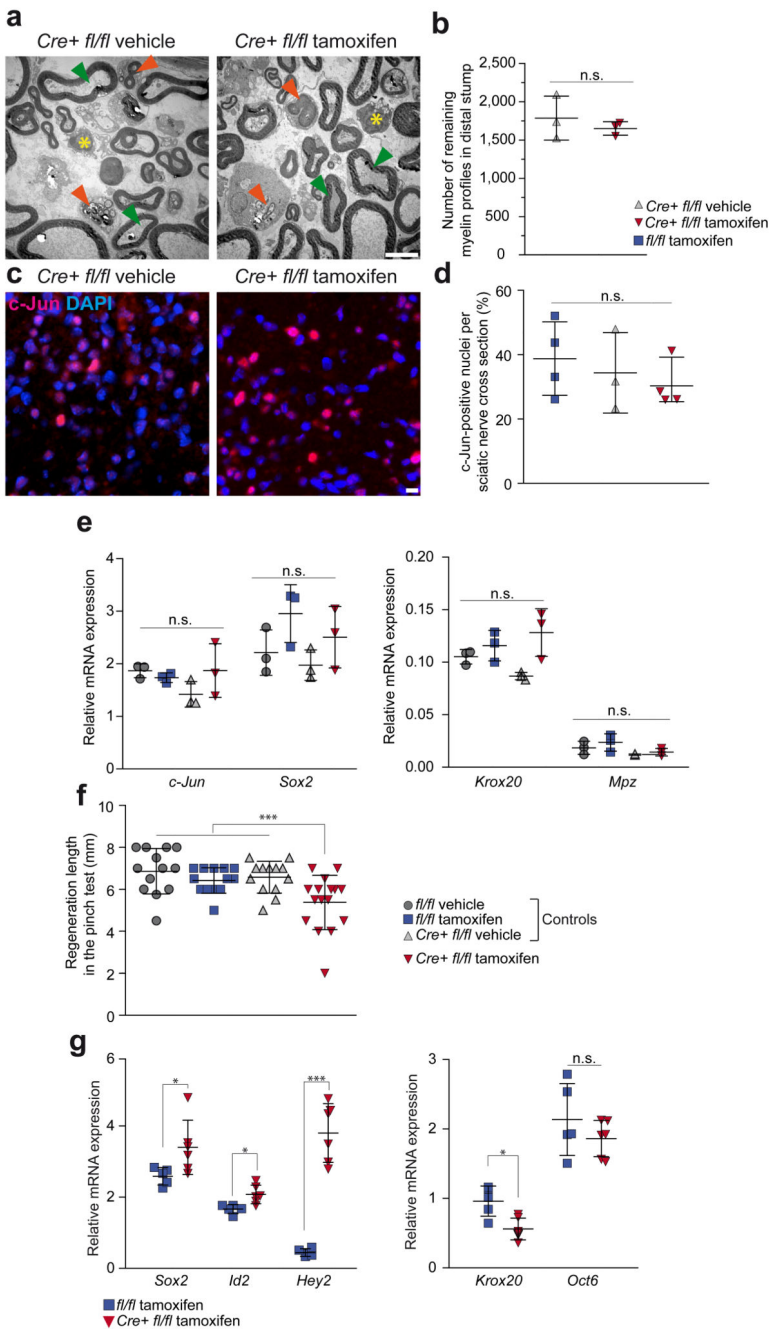

Figure 7. Dedifferentiation and redifferentiation of Zeb2-deficient Schwann cells

(a) Imaged 3 days after sciatic nerve transection (dedifferentiation), the amount of myelin debris (orange arrow heads) and residual myelin profiles (green arrow heads) appears similar in the distal nerve segment of (vehicle-treated) controls (left panel) and tamoxifen-treated *PLP-creERT2::Zeb2*$^{fl/fl}$ mutants (right panel). Yellow asterisks: invading macrophages. Scale bar, 5 μm. Representative images of 3 mice per group.

(b) When quantified in the distal sciatic nerve stump, the number of residual myelin profiles is not different (each dot represents 1 individual animal ±SD, P=0.50456, t=0.7819589, n=3 mice per group, two-sided student's t-test of unpaired samples, n.s. not significant).
(c) Nuclear c-Jun immunofluorescence on cross sections of the distal sciatic nerve segment 3 days after nerve crush shows a similar number of dedifferentiating Schwann cells (c-Jun: pink, DAPI: blue, the experiment was repeated successfully on sections of 4 mice per group, except for Cre+ fl/fl vehicle n=3, scale bar, 5 μm).
(d) Quantification of c-Jun-positive nuclei on sections of the distal sciatic nerve segment 3 days after nerve crush as depicted in **(c)** shows a similar number for tamoxifen-treated *PLP-creERT2::Zeb2*$^{fl/fl}$ mutants and two corresponding control groups (n=4 mice per group, except for Cre+ fl/fl vehicle n=3, each dot represents one individual animal ±SD, one-way ANOVA P=0.5366, F(2,8)=0.6735603).
(e) After 3 days, normal Schwann cell dedifferentiation is also suggested by the elevated steady-state levels of c-Jun and Sox2 mRNAs. Krox20 and Mpz mRNAs were similarily downregulated in all groups. Expression in the contralateral nerve was defined as 1.0. Each dot represents sciatic nerve mRNA from 1 individual mouse with cross lines at the mean ±SD (n=3 mice per group, Kruskal-Wallis one-way ANOVA, c-Jun: P=0.1473, H=5.358974, Sox2: P=0.1319, H=5.615385, Krox20: P=0.0572, H=7.512821, Mpz: P=0.1129, H=5.974, n.s. not significant).
(f) Delayed functional recovery of sciatic nerves after crush, as assessed by the "pinch test" reflecting axon regrowth. In tamoxifen-treated *PLP-creERT2::Zeb2*$^{fl/fl}$ mice (in red) regenerative length 4 days after nerve crush does not reach various control values (in grey/blue). Each dot represents the regeneration distance of 1 individual mouse with cross lines at the mean ±SD (n=13 mice per group except fl/fl tamoxifen: n=16, one-way ANOVA P=0.001, F(3,51)=6.356539, *** P=0.001).
(g) After 56 days, levels of Sox2 and Id2 were strongly upregulated in injured nerves, but even more so in tamoxifen-treated *PLP-creERT2::Zeb2*$^{fl/fl}$ mutant mice. *Hey2* levels were downregulated in injured control nerves, but highly upregulated in tamoxifen-treated *PLP-creERT2::Zeb2*$^{fl/fl}$ mutant mice. *Krox20* levels remained low in nerves of mutants, while *Oct6* was still upregulated to comparable levels in both genotypes. Each dot represents cDNA from 1 individual mouse run in triplicate ±SD with cross lines at the mean. Expression in the contralateral nerve was defined as 1.0. (Cre+ fl/fl tamoxifen: n=6; fl/fl tamoxifen: n=5; contralateral, n=5, Sox2: P=0.0493, t=2.271339, Id2: P=0.0109, t=3.197971, Hey2: P=0.00072063, t=8.963330, Krox20: P=0.0062, t=3.547758, Oct6:P=0,2807, t=1.147759, * P <0.05; *** P <0.001, n.s. not significant).